Cell Reports

Article

The Cdc48 Complex Alleviates the Cytotoxicity of Misfolded Proteins by Regulating Ubiquitin Homeostasis

Graphical Abstract

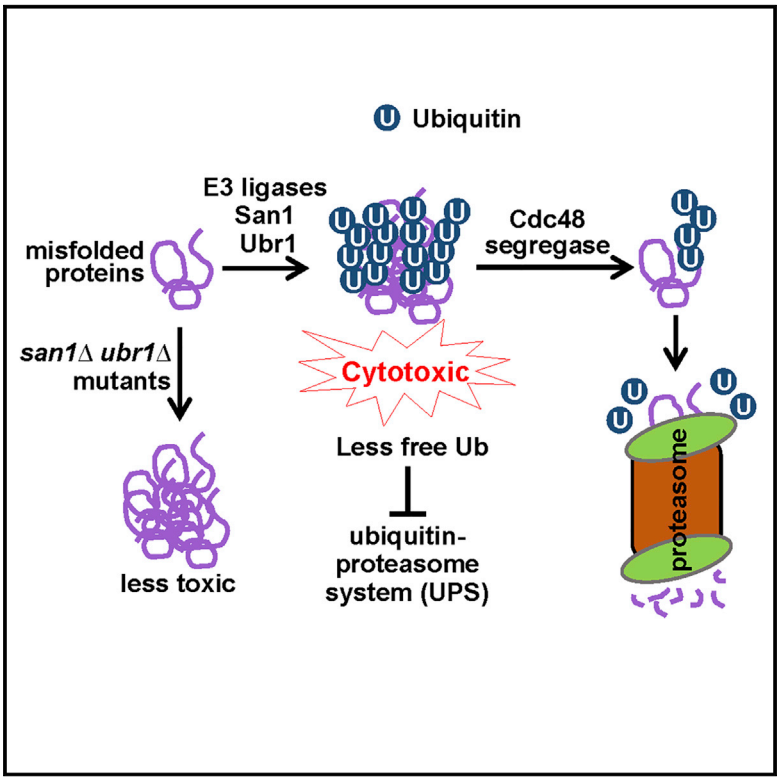

Authors

Ryan Higgins, Marie-Helene Kabbaj, Delaney Sherwin, Lauren A. Howell, Alexa Hatcher, Robert J. Tomko, Jr., Yanchang Wang

Correspondence

yanchang.wang@med.fsu.edu

In Brief

Misfolded protein accumulation causes cytotoxicity, but the mechanism remains poorly understood. Using budding yeast as a model organism, Higgins et al. show that ubiquitination of misfolded proteins depletes free ubiquitin, which compromises ubiquitin-dependent cellular functions and causes cytotoxicity. The Cdc48/p97 segregase antagonizes this cytotoxicity by promoting ubiquitin recycling from misfolded proteins.

Highlights

- Cdc48 segregase is required for the degradation of misfolded proteins in yeast
- Cdc48 deficiency leads to a decreased pool of free ubiquitin that compromises the UPS
- San1 and Ubr1 ubiquitinate misfolded proteins, reducing the free ubiquitin pool
- Restoring free ubiquitin suppresses the toxicity associated with Cdc48 deficiency

Higgins et al., 2020, Cell Reports *32*, 107898
July 14, 2020
https://doi.org/10.1016/j.celrep.2020.107898

CellPress

Cell Reports

CellPress
OPEN ACCESS

Article

The Cdc48 Complex Alleviates the Cytotoxicity of Misfolded Proteins by Regulating Ubiquitin Homeostasis

Ryan Higgins,[1,3] Marie-Helene Kabbaj,[1] Delaney Sherwin,[1] Lauren A. Howell,[1] Alexa Hatcher,[2] Robert J. Tomko, Jr.,[1] and Yanchang Wang[1,4,*]

[1]Department of Biomedical Sciences, College of Medicine, Florida State University, 1115 West Call Street, Tallahassee, FL 32306, USA
[2]College of Nursing, Florida State University, 600 West College Avenue, Tallahassee, FL 32306, USA
[3]Present address: Department of Pathology and Laboratory Medicine, Indiana University School of Medicine, Indianapolis, IN 46202, USA
[4]Lead Contact
*Correspondence: yanchang.wang@med.fsu.edu
https://doi.org/10.1016/j.celrep.2020.107898

SUMMARY

The accumulation of misfolded proteins is associated with multiple neurodegenerative disorders, but it remains poorly defined how this accumulation causes cytotoxicity. Here, we demonstrate that the Cdc48/p97 segregase machinery drives the clearance of ubiquitinated model misfolded protein Huntingtin (Htt103QP) and limits its aggregation. Nuclear ubiquitin ligase San1 acts upstream of Cdc48 to ubiquitinate Htt103QP. Unexpectedly, deletion of *SAN1* and/or its cytosolic counterpart *UBR1* rescues the toxicity associated with Cdc48 deficiency, suggesting that ubiquitin depletion, rather than compromised proteolysis of misfolded proteins, causes the growth defect in cells with Cdc48 deficiency. Indeed, Cdc48 deficiency leads to elevated protein ubiquitination levels and decreased free ubiquitin, which depends on San1/Ubr1. Furthermore, enhancing free ubiquitin levels rescues the toxicity in various Cdc48 pathway mutants and restores normal turnover of a known Cdc48-independent substrate. Our work highlights a previously unappreciated function for Cdc48 in ensuring the regeneration of monoubiquitin that is critical for normal cellular function.

INTRODUCTION

Correct folding of proteins is essential for their function. Although protein folding is a tightly regulated process, misfolded proteins are still generated within cells for various reasons. Low levels of protein misfolding occur spontaneously, but gene mutations, translational errors, aging, and various chemical stressors escalate protein misfolding (Tyedmers et al., 2010). The accumulation of misfolded proteins is associated with multiple neurodegenerative disorders, including Alzheimer's and Huntington diseases (Knowles et al., 2014; Soto, 2003). In addition, protein misfolding has been implicated in diabetes and cancer (de Oliveira et al., 2015; Mukherjee et al., 2015). Unfortunately, why misfolded proteins are cytotoxic and how cells counteract this toxicity remain poorly understood.

Misfolded proteins are prone to aggregation due to exposed hydrophobic surfaces. The association between hydrophobic domains results in amorphous aggregates. These amorphous aggregates are oligomeric and mostly below the detection limit by microscopy (nm size) (Mogk et al., 2018). An increased concentration of misfolded proteins leads to the formation of microscopically detectable inclusion bodies (μm size) (Hipp et al., 2012; Mogk et al., 2018). Oligomeric aggregates (hereafter, aggregates) are potentially cytotoxic and may contribute to cytotoxicity by sequestrating transcription factors, RNA, and chaperones or by causing endoplasmic reticulum stress (Hartl et al., 2011; Leitman et al., 2013; Ogen-Shtern et al., 2016; Yang and Hu, 2016). However, a more general mechanism likely contributes to the toxicity of misfolded protein aggregates.

Misfolded proteins can be refolded with the assistance of molecular chaperones. They can also be degraded by the ubiquitin-proteasome system (UPS) or by the autophagy pathway. The sequential actions of E1 ubiquitin-activating, E2 ubiquitin-conjugating, and E3 ubiquitin-ligase enzymes covalently attach a polyubiquitin chain to misfolded substrates, which targets them to the proteasome for degradation (Finley et al., 2012). Among the dozens of ubiquitin ligases in budding yeast, San1 and Ubr1 are responsible for the ubiquitination and degradation of misfolded proteins. San1 is the predominant ubiquitin ligase involved in nuclear substrate ubiquitination (Dasgupta et al., 2004; Gardner et al., 2005), whereas cytosolic misfolded proteins are mainly ubiquitinated by Ubr1 (Eisele and Wolf, 2008; Samant et al., 2018). The E3 ligase Ubr1 relies on chaperones to detect and bind misfolded substrates, but San1 appears to bind directly to a wide variety of misfolded proteins (Heck et al., 2010; Rosenbaum et al., 2011). Misfolded protein aggregates require enzymes for disaggregation and the subsequent refolding or degradation. Yeast cells utilize the AAA+ (ATPase associated with various cellular activities) chaperone Hsp104 as a powerful disaggregase (Miller et al., 2015). Hsp104 contains

a hydrophobic pocket in its N-terminal domain that interacts with substrates (Aguado et al., 2015).

Yeast cells also utilize a conserved AAA ATPase, Cdc48 (p97/VCP in metazoans), to separate proteins from one another and thus has been termed a segregase. Cdc48 is composed of an N-terminal domain, two centrally located ATPase domains, and a C-terminal tail. Six Cdc48 monomers form a double-ring structure surrounding a central pore (Bodnar and Rapoport, 2017b). This homohexameric structure, along with the help of cofactors, extracts polyubiquitinated substrates from membranes and macromolecular complexes, which facilitates protein relocalization or proteasomal degradation (Bodnar and Rapoport, 2017a). Recent *in vitro* evidence indicates that the Cdc48 complex acts as an unfoldase to generate unstructured ubiquitin or segments for its substrates (Olszewski et al., 2019; Twomey et al., 2019). The prominent cofactors for Cdc48, Npl4 and Ufd1, contain ubiquitin binding domains (Bodnar et al., 2018). The $Cdc48^{Ufd1/Npl4}$ complex is involved in chromatin remodeling, DNA replication, endoplasmic-reticulum-associated degradation (ERAD), selective autophagy, and membrane fusion (Ye et al., 2017). However, the segregase function of Cdc48 in response to proteotoxic stress remains poorly defined.

Ubiquitin exists in the cells as monomers (free ubiquitin) or as chains, most of which are covalently attached to other proteins. The balance between these two pools (ubiquitin homeostasis) is tightly regulated by the antagonistic actions of ubiquitin ligases, which assemble chains, and deubiquitinating enzymes, which disassemble them (Komander et al., 2009; Reyes-Turcu et al., 2009). In yeast, deubiquitinase Doa4 controls the free ubiquitin level by recycling polyubiquitin, and *doa4*Δ cells exhibit free ubiquitin depletion and hypersensitivity to proteotoxic stressors (Swaminathan et al., 1999). Rfu1, a negative regulator of Doa4, was identified as a high-copy suppressor of the *cdc48-3* mutant, indicating that Cdc48 might be involved in ubiquitin homeostasis (Kimura et al., 2009). However, the function of Cdc48 in ubiquitin homeostasis and the response to proteotoxic stress remain unclear. Here, we present data suggesting that the ubiquitination of misfolded proteins causes cytotoxicity by draining free ubiquitin and compromising UPS function. The Cdc48 complex combats this toxic effect by disaggregating ubiquitinated protein aggregates, which facilitates ubiquitin recycling and UPS-mediated protein degradation. These observations shed light on the molecular basis for the cytotoxicity of misfolded proteins, as well as the critical role of the $Cdc48^{Ufd1/Npl4}$ complex in alleviating this toxicity.

RESULTS

The $Cdc48^{Ufd1/Npl4}$ Complex Is Essential for Proteasomal Degradation of Mutant Huntingtin

The $Cdc48^{Ufd1/Npl4}$ complex extracts polyubiquitinated proteins from membranes or macromolecular complexes (Bodnar and Rapoport, 2017b). In yeast cells, Cdc48 has been shown to associate with mutated Huntingtin proteins containing a polyQ expansion and a proline-rich region (Htt103QP) (Wang et al., 2009). More recently, p97, the human homolog of Cdc48, was shown to colocalize with mutated Huntingtin in mammalian cells and exhibit segregase activity (Ghosh et al., 2018). Because our previous work shows that Htt103QP is readily degraded and proteasome inhibitor MG132 blocks this degradation (Chuang et al., 2016; Higgins et al., 2018), we tested if the $Cdc48^{Ufd1/Npl4}$ complex promotes proteasomal degradation of Htt103QP. For this purpose, we induced FLAG-Htt103QP-GFP expression in wild-type (WT) and *cdc48-3* cells from a galactose-inducible promoter (GAL) for 1 h before shutoff by adding glucose. At the semi-permissive temperature 34°C, we observed significant stabilization of Htt103QP in *cdc48-3* mutant cells, but WT cells showed very efficient Htt103QP degradation. Mutation of the Cdc48 cofactors Npl4 and Ufd1 also caused a significant delay in Htt103QP degradation (Figure 1A). We further compared Htt103QP stability in WT and *cdc48-3* mutant cells after protein synthesis inhibition by cycloheximide. Impaired Htt103QP degradation was also observed in *cdc48-3* cells by using the cycloheximide chase method (Figure 1B). The expression of mutated Huntingtin lacking the flanking proline-rich region (Htt103QΔP) in yeast cells alters the shape and number of inclusions and causes cytotoxicity (Dehay and Bertolotti, 2006). Compared to Htt103QP, the degradation of Htt103QΔP was much less efficient, and Htt103QΔP overexpression led to the formation of numerous inclusion bodies in each yeast cell (Figure S1). These results indicate an essential role for the $Cdc48^{Ufd1/Npl4}$ complex in proteasomal degradation of Htt103QP and that the flanking proline-rich region is critical for Htt103QP degradation.

The impaired degradation of Htt103QP in *cdc48* mutants could be a result of defective Htt103QP ubiquitination. To test this possibility, FLAG-Htt103QP-GFP was immunoprecipitated from protein extracts prepared using WT, *cdc48-3*, *npl4-1*, and *ufd1-2* mutant cells after a 3-h galactose induction of Htt103QP at 34°C. Htt103QP ubiquitination was then examined with an anti-ubiquitin antibody. We observed a much stronger accumulation of ubiquitinated Htt103QP in all the mutants compared to WT cells (Figure 1C), suggesting that the functional Cdc48 complex is essential for the degradation of mutated Huntingtin but is dispensable for its ubiquitination.

San1 Ubiquitinates Htt103QP for Proteasomal Degradation

We next sought to determine which E3 ubiquitin ligase(s) is responsible for Htt103QP ubiquitination and degradation. E3 ligase Ltn1 promotes the ubiquitination of mutant Huntingtin in yeast cells (Yang et al., 2016). However, no significant difference was detected for Htt103QP degradation efficiency between WT and *ltn1Δ* cells (Figure 2A), indicating that a different or additional E3 ligase catalyzes Htt103QP ubiquitination. To identify the ligase(s), we assessed Htt103QP degradation in 71 yeast strains that each carried a deletion of a verified or putative ubiquitin ligase gene (Table S1; Fang et al., 2011). As described previously (Chuang et al., 2016), a haploid strain containing P_{GAL}*FLAG-Htt103QP-GFP* was crossed with these 71 deletion mutants. Diploids were selected and sporulated and then haploid strains containing P_{GAL}*FLAG-Htt103QP-GFP* and a ubiquitin ligase deletion were isolated. We examined Htt103QP protein stability in these mutants after galactose induction of Htt103QP for 1 h and followed by expression shutoff with glucose for 3 h. Of the 71 tested mutants, only deletion of

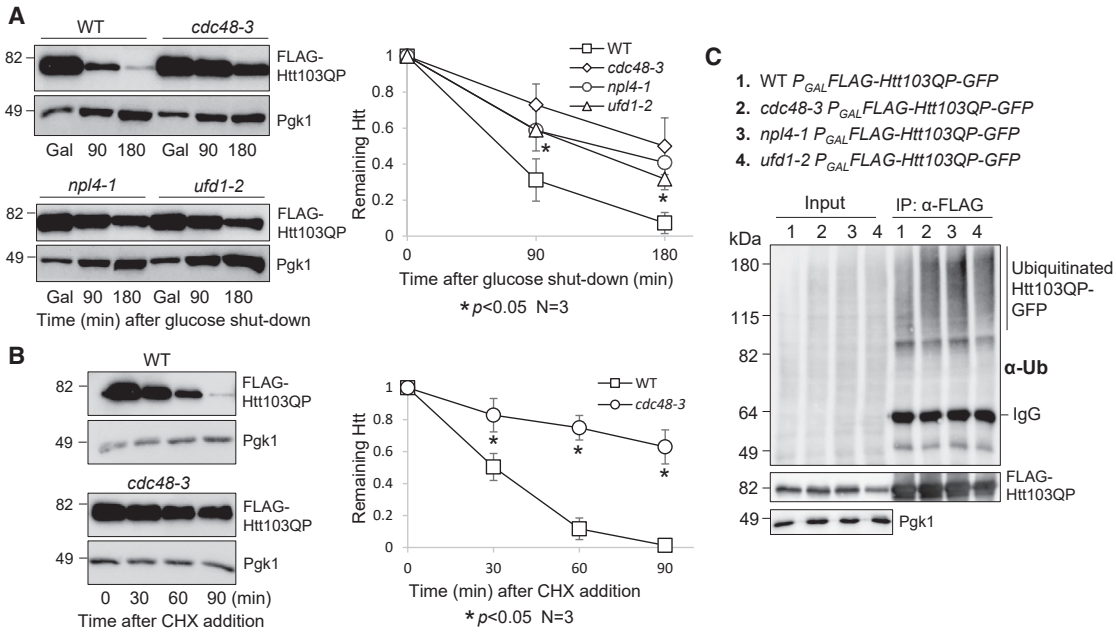

Figure 1. The Cdc48$^{Npl4/Ufd1}$ Complex Is Required for Htt103QP Degradation but Is Dispensable for Its Ubiquitination

(A) The degradation of Htt103QP depends on the Cdc48$^{Npl4/Ufd1}$ complex. WT (3419-1-1), *cdc48-3* (3598-2-3), *npl4-1* (3387-3-4), and *ufd1-2* (3385-4-4) mutants containing an integrating plasmid, *P_{GAL}FLAG-Htt103QP-GFP*, were grown in non-inducing raffinose medium (YPR) to mid-log phase at 25°C. Galactose was added to the medium (2% final concentration) for 50 min to induce FLAG-Htt103QP-GFP expression at 25°C. Cells were then shifted to 34°C for 10 additional min, and glucose was added to shut off the expression. FLAG-Htt103QP-GFP protein levels were detected using anti-FLAG antibody. Pgk1, loading control. The levels of Htt103QP and Pgk1 are shown on the left. The intensity of protein bands and the Htt103QP/Pgk1 ratio were analyzed using ImageJ. The remaining Htt103QP after glucose shutoff was calculated based on the results from three independent experiments. The results are represented as mean ± SD (standard deviation). Wilcoxon rank-sum test was used to calculate the p values. The statistical difference is significant (*) when $p < 0.05$.

(B) Impaired Htt103QP degradation was estimated by cycloheximide (CHX) chase. WT (3419-1-1) and *cdc48-3* (3598-2-3) strains with *P_{GAL}FLAG-Htt103QP-GFP* were grown in YPR at 25°C to mid-log phase. Galactose was added to the medium for 30 min, followed by temperature shift to 34°C for 30 min. Then, CHX (200 μg/mL) was added, and the protein levels of Htt103QP and Pgk1 were determined over time. The experiment was repeated three times. Quantification of the Htt103QP/Pgk1 ratio and statistical analysis were performed as described above, and the relative levels of Htt103QP to Pgk1 are represented as mean ± SD. *$p < 0.05$.

(C) Cdc48 is not required for Htt103QP ubiquitination. WT (3419-1-1), *cdc48-3* (3598-2-3), *npl4-1* (3387-3-4), and *ufd1-2* (3385-4-4) mutant cells containing *P_{GAL}FLAG-Htt103QP-GFP* were grown in YPR to mid-log phase at 25°C. Galactose was then added, and cells were shifted to 34°C for 3 h. The protein extracts were prepared as described in the STAR Methods. FLAG-Htt103QP-GFP was immunoprecipitated using M2 anti-FLAG beads. Htt103QP protein levels were detected using an anti-FLAG antibody, and protein ubiquitination was detected using anti-Ub antibody. Pgk1, loading control.

SAN1, a nuclear ubiquitin ligase that promotes the ubiquitination of misfolded proteins (Heck et al., 2010; Samant et al., 2018), resulted in obvious Htt103QP stabilization (Figure 2A). Ubr1 ubiquitin ligase localizes in the cytoplasm to ubiquitinate misfolded proteins and thereby acts as the cytosolic equivalent of San1. Unexpectedly, no significant Htt103QP stabilization was detected in *ubr1*Δ mutant cells. In addition, the absence of Ufd2, a ligase that synthesizes branched ubiquitin chains (Liu et al., 2017), had a much less severe but statistically significant defect in Htt103QP degradation that was evident at longer time points (Figure 2A). Therefore, these results support the conclusion that San1 E3 ligase plays a critical role for Htt103QP degradation.

We further determined the role of San1 in the ubiquitination of Htt103QP. We found that *san1*Δ mutant cells exhibited a dramatic decrease in Htt103QP ubiquitination (Figure 2B). Of note, some ubiquitination of Htt103QP was detected in *san1⊿* cells, which is likely attributable to other E3 ligases. To the point, a previous study shows a defect in Htt103QP ubiquitination in yeast mutants lacking E3 ligase Ltn1 (Yang et al., 2016). Moreover, ubiquitin ligase Rsp5 has been shown to catalyze the ubiquitination of Htt96Q (mutated Htt with 96 polyQ repeats) in yeast cells (Lu et al., 2014). Unlike the Htt103QP protein, Htt96Q lacks the proline-rich region. Regardless, the dramatic defect in Htt103QP ubiquitination and degradation in *san1*Δ cells suggest that San1 plays a major role in the ubiquitination of mutated Huntingtin in yeast cells.

Htt103QP forms inclusion bodies in yeast cells when it is overexpressed (Chuang et al., 2016; Higgins et al., 2018; Wang et al., 2009). We found that in *san1⊿* cells, Htt103QP inclusion bodies formed at an accelerated rate compared to WT cells after Htt103QP induction in galactose medium (Figure 2C). In addition, many *san1⊿* cells had two or more inclusion bodies after Htt103QP induction, but very few WT cells showed more than one inclusion body. These results suggest that ubiquitination of Htt103QP by San1 is not necessary for its recruitment to inclusion bodies, which is consistent with previous observations in mammalian cells (Bersuker et al., 2016). Because the E3 ligase

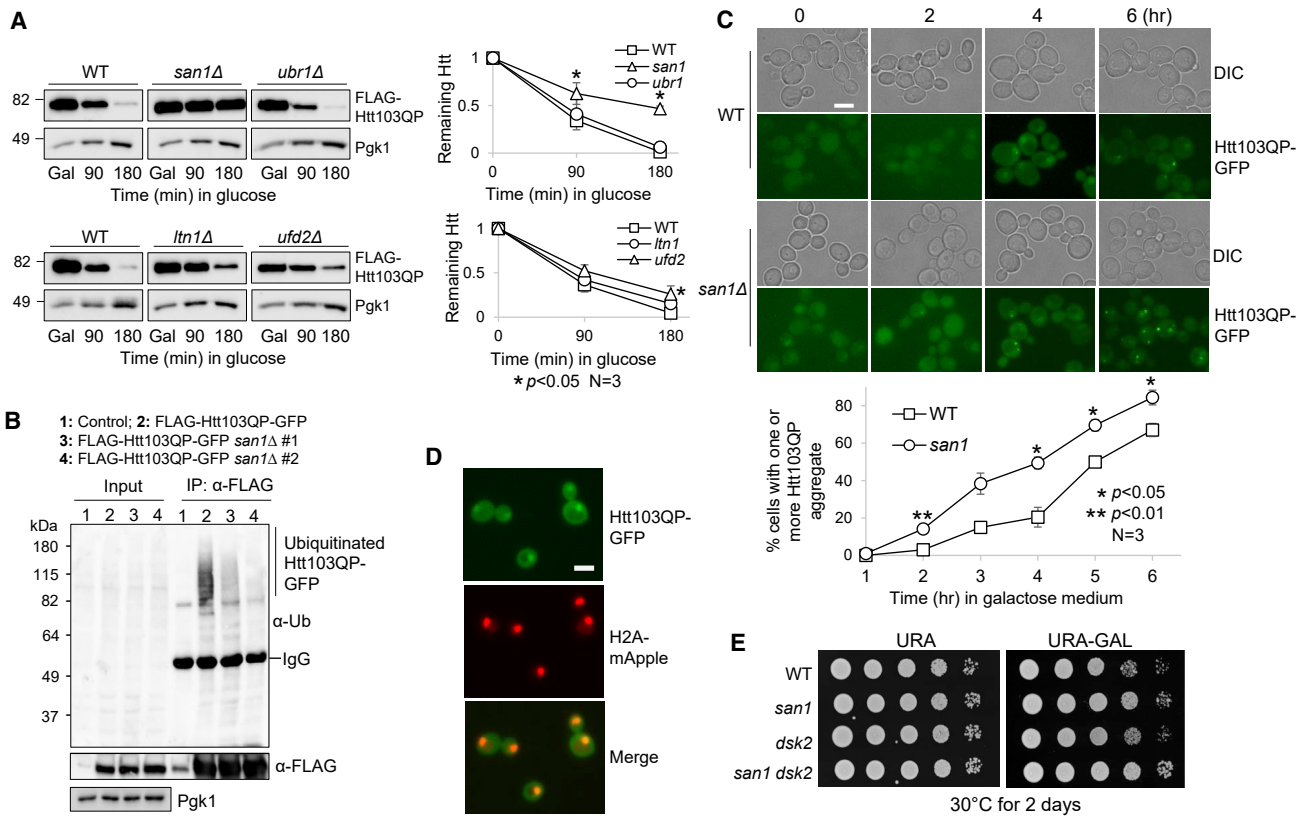

Figure 2. E3 Ubiquitin Ligase San1 Ubiquitinates Htt103QP for Degradation

(A) San1 is required for Htt103QP degradation. WT (3419-1-1), *san1Δ* (RH142), *ubr1Δ* (3522-4-4), *ltn1*Δ (3287-1-1), and *ufd2*Δ (3288-1-3) cells containing P_{GAL}*FLAG-Htt103QP-GFP* were grown in YPR to mid-log phase at 30°C. Galactose was then added to induce Htt103QP expression for 1 h. Glucose was then added to shut off galactose-induced expression. Htt103QP protein levels were detected using an anti-FLAG antibody. The experiment was repeated three times. The western blotting result for Htt103QP level is shown on the left panel. Pgk1, loading control. Protein band intensity and Htt103QP/Pgk1 ratio were analyzed using ImageJ. Quantification results are represented as mean ± SD (right panel). * indicates statistical significant ($p < 0.05$).

(B) San1 promotes ubiquitination of Htt103QP. WT (3419-1-1) and two *san1Δ* mutant strains (RH142 and 3301-2-2) containing P_{GAL}*FLAG-Htt103QP-GFP* were grown in YPR to mid-log phase at 30°C. Galactose was then added to induce Htt103QP overexpression for 3 h. After preparation of cell lysates, Htt103QP was immunoprecipitated using M2 anti-FLAG beads. Htt103QP protein levels were detected using anti-FLAG antibody, and the ubiquitination level was detected using anti-Ub antibody. Pgk1, loading control.

(C) Htt103QP inclusion bodies form at an accelerated rate in *san1Δ* mutant. WT (3419-1-1) and *san1Δ* (RH142) cells containing P_{GAL}*FLAG-Htt103QP-GFP* were grown in YPR to mid-log phase at 30°C. Galactose was then added to induce Htt103QP expression. Differential interference contrast (DIC) and GFP fluorescence images were obtained every h for 6 h. Scale bar, 5 μm. The quantitative result is the average from three independent experiments. Data are represented as mean ± SD. Two-way ANOVA with Tukey's multiple comparisons test was performed for each dataset. *$p < 0.05$.

(D) Htt103QP shows nuclear localization. Yeast cells with *H2A-mApple* and P_{GAL}*FLAG-Htt103QP-GFP* (2925-3-2) were grown in YPR, and then galactose was added to induce Htt103QP expression. Images were acquired after incubation in galactose for 1 h. Scale bar, 5 μm.

(E) Cells lacking *SAN1* are not sensitive to Htt103QP overexpression. WT (3419-1-1), *san1Δ* (3301-2-2), *dsk2*Δ (3222-1-1), and *dsk2*Δ *san1*Δ (3514-1-2) strains with P_{GAL}*FLAG-Htt103QP-GFP* were grown to saturation in YPR, and then 10-fold serially diluted and spotted onto URA (uracil) dropout plates containing glucose or galactose. The plates were incubated at 30°C for 2 days.

San1 localizes in the nucleus, the nuclear localization of Htt103QP is likely required for its ubiquitination by San1. After Htt103QP-GFP induction for 1 h, before inclusion bodies had formed, we detected colocalization of Htt103QP-GFP with histone H2A-mApple, which marks the nucleus (Figure 2D). In spite of the stabilization of Htt103QP in *san1Δ* mutants, *san1Δ* cells grew slightly better than WT cells on galactose plates that induced Htt103QP overexpression. We found that deletion of the ubiquilin ortholog *DSK2* in yeast cells resulted in sensitivity to Htt103QP overexpression (Chuang et al., 2016), but this sensitivity was abolished in *dsk2*Δ *san1*Δ cells (Figure 2E), indicating that high levels of un-modified Htt103QP is not cytotoxic. Taken together, these results suggest that E3 ubiquitin ligase San1 ubiquitinates Htt103QP-GFP and targets it for proteasomal degradation, whereas defective ubiquitination of Htt103QP leads to accelerated inclusion body formation with no accompanying cytotoxicity.

San1- and Ubr1-Dependent Ubiquitination Causes Cytotoxicity in *cdc48* Mutant Cells

Considering that both San1 and the $Cdc48^{Ufd1/Npl4}$ complex promote Htt103QP degradation and that San1 is the major E3 ligase

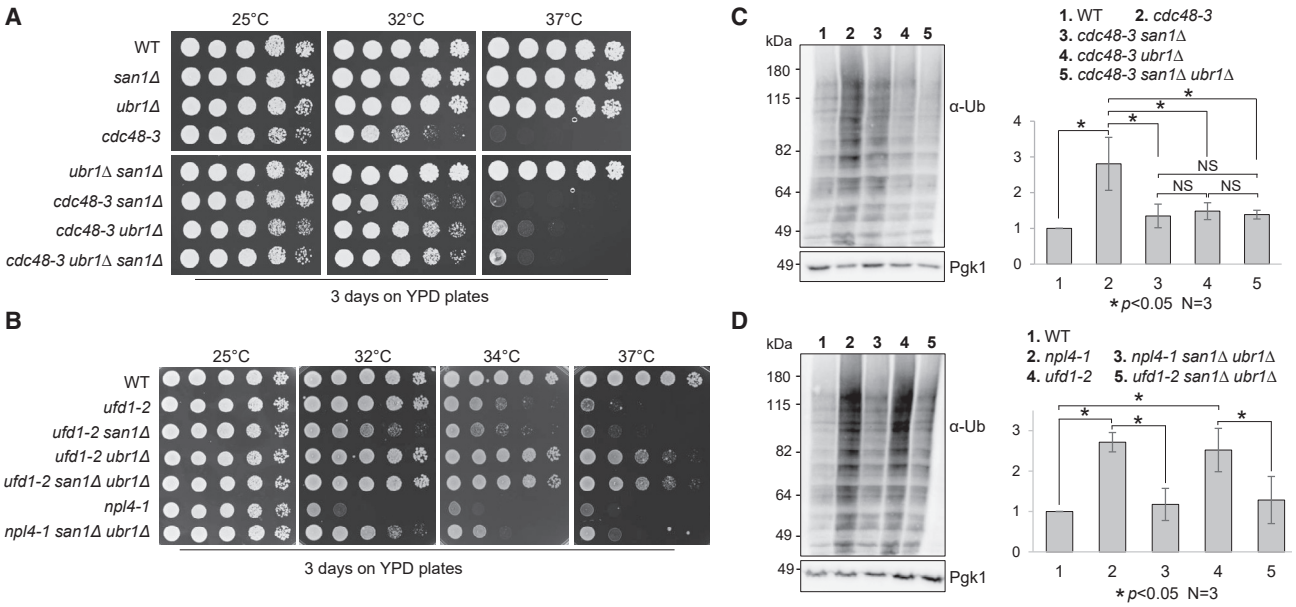

Figure 3. The Absence of San1 and Ubr1 Partially Suppresses the Temperature Sensitivity of *cdc48-3*, *npl4-1*, and *ufd1-2* Mutants

(A) The suppression of the temperature sensitivity of *cdc48-3* mutants by *san1Δ*, *ubr1Δ*, and *san1Δ ubr1Δ* mutants. Cells with the indicated genotypes were grown in YPD to saturation and then 10-fold serially diluted onto YPD plates. The plates were incubated at 25°C, 32°C, and 37°C for 2 days. Strains used in this experiment were WT (Y300), *cdc48-3* (MHY3512), *cdcc48-3 san1*Δ (3550-5-3), *cdc48-3 ubr1*Δ (3550-6-3), and *cdc48-3 san1Δ ubr1*Δ (3550-2-1).

(B) The growth defect of *npl4-1* and *ufd1-2* is partially suppressed by *san1Δ ubr1Δ* mutants. The strains used were WT (Y300), *ufd1-2* (1122), *ufd1-2 san1Δ* (3556-1-1), *ufd1-2 ubr1*Δ (3556-2-3), *ufd1-2 san1Δ ubr1*Δ (3556-3-3), *npl4-1* (1126), and *npl4-1 san1*Δ *ubr1*Δ (3555-5-1). The plates were incubated at 25°C, 32°C, 34°C, and 37°C for 2 days.

(C) The accumulation of ubiquitinated proteins in *cdc48-3* mutant cells is suppressed by *san1Δ*, *ubr1Δ*, and *san1Δ ubr1Δ* mutants. Cells with the indicated genotypes were grown in YPD at 25°C and then shifted to 34°C for 5 h. Protein samples were prepared, and ubiquitinated protein species were detected using an anti-Ub antibody. Pgk1, loading control. The experiment was repeated three times. The band intensity of ubiquitinated protein species and Pgk1 was analyzed using ImageJ. The relative ubiquitination level over Pgk1 is shown as mean ± SD. *p < 0.05. NS, not statistically significant. Strains used in this experiment were WT (Y300), *cdc48-3* (MHY3512), *cdc48-3 san1*Δ (3550-5-3), *cdc48-3 ubr1*Δ (3550-6-3), and *cdc48-3 san1Δ ubr1*Δ (3550-2-1).

(D) The accumulation of ubiquitinated proteins in *npl4* and *ufd1* mutants is suppressed by *san1Δ ubr1Δ*. Quantification of relative level of protein ubiquitination and statistical analysis were performed as described above. The strains used in this experiment were WT (Y300), *npl4-1* (1126), *npl4-1 san1*Δ *ubr1*Δ (3555-5-1), *ufd1-2* (1122), and *ufd1-2 san1Δ ubr1*Δ (3556-3-3).

that ubiquitinates Htt103QP, we speculated that San1-dependent ubiquitination of Htt103QP and other misfolded proteins in the nucleus enables Cdc48-mediated dissolution of protein aggregates. Therefore, the combination of *SAN1* deletion and *cdc48* mutation may exacerbate protein aggregation and cause proteotoxicity. Surprisingly, the growth defect of *cdc48-3* at elevated temperatures (32°C) was partially suppressed by *san1Δ* (Figure 3A). E3 ligase Ubr1 is the cytosolic counterpart of San1. Compared to the *san1*Δ mutant, *ubr1Δ* had a more profound suppression of the *cdc48-3* growth defects at 32°C, and the suppression was even noticeable at 37°C. Similarly, the suppression of the temperature sensitivity of *ufd1-2* mutants by *ubr1Δ* was more dramatic than *san1Δ*. Strikingly, the growth defect of *ufd1-2* at 37°C was near-completely suppressed by *ubr1Δ* and *san1Δ ubr1Δ*. We also observed the suppression of the temperature sensitivity of the *npl4-1* mutant by *san1Δ ubr1Δ* at 32°C and 34°C (Figure 3B). Therefore, San1/Ubr1-dependent ubiquitination of misfolded proteins likely contributes to the growth defect in cells with $Cdc48^{Ufd1/Npl4}$ deficiency, and Ubr1-dependent ubiquitination of misfolded proteins in the cytoplasm seems to play a more important role.

Downregulation of Cdc48 results in significant accumulation of polyubiquitinated proteins in *Drosophila*, zebrafish, and human cells (Imamura et al., 2012). We tested if yeast *cdc48* mutants accumulate more ubiquitinated proteins and if this accumulation depends on San1 and Ubr1. When grown at 34°C, *cdc48-3* mutants exhibited a much higher level of ubiquitinated protein species than did WT cells. Strikingly, deletion of *SAN1*, *UBR1*, or *SAN1 UBR1* strongly suppressed this accumulation, and the suppression was statistically significant. Although the suppression of the temperature sensitivity by *ubr1*Δ was more profound than *san1*Δ, we did not observe stronger suppression of the accumulation of ubiquitinated protein species in *cdc48-3* by *ubr1*Δ or *san1*Δ *ubr1*Δ than *san1*Δ (Figure 3C). One explanation is that the ubiquitinated misfolded proteins in the nucleus or cytoplasm exhibit different toxicity. Similarly, a dramatic increase in ubiquitinated protein species was detected in *npl4-1* and *ufd1-2* mutants grown at 34°C, and this accumulation was abolished by *san1*Δ *ubr1*Δ (Figure 3D). These results suggest that most $Cdc48^{Ufd1/Npl4}$ substrates are ubiquitinated by San1 and Ubr1 E3 ligases.

Given that San1 and Ubr1 ubiquitinate misfolded proteins that are prone to aggregation, cells with Cdc48 deficiency might accumulate more misfolded protein aggregates. To test this idea, we used C-terminally GFP-tagged Hsp104, a disaggregase chaperone, to mark endogenous protein aggregates (Higgins et al., 2018; Jacobson et al., 2012). After shifting the temperature from 25°C to 34°C for 1 h, both WT and *cdc48-3* cells exhibited an initial increase in the number of Hsp104-GFP foci, presumably due to heat shock. The average number of GFP foci in WT cells was approximately one focus per cell, but the average number was over three in *cdc48-3* cells. After 3 h at 34°C, the number of Hsp104-GFP foci in WT cells decreased but remained relatively constant in *cdc48-3* cells (Figure S2A). Similarly, an increase in Hsp104-GFP foci was also observed in the *npl4-1* and *ufd1-2* mutant cells growing at 34°C (Figure S2B). Because the foci appear similar in size in WT and mutant cells, these results suggest that compromised $Cdc48^{Ufd1/Npl4}$ function results in the accumulation of more protein aggregates due to a reduced efficiency of clearance.

Impairment of the UPS in *cdc48-3* Mutants

Our results suggest that San1/Ubr1-dependent ubiquitination of misfolded proteins partially contributes to the growth defect in cells with Cdc48 deficiency. One further question is how the ubiquitination of misfolded proteins contributes to the growth defect in *cdc48* mutant cells. One possibility is that the ubiquitination of large amounts of misfolded proteins compromises UPS function by occupying and potentially inhibiting proteasomes. Alternatively, this ubiquitination results in the depletion of free ubiquitin necessary for UPS function and/or other cellular processes. To test this idea, we first used genetic methods to examine the UPS function in the *cdc48-3* mutant. Rpn4 is a transcription factor, and *RPN4* deletion compromises UPS function by downregulating the expression of proteasome subunits (Xie and Varshavsky, 2001). We crossed *rpn4Δ* with *cdc48-3*, but after tetrad dissection, no *rpn4Δ cdc48-3* double mutants were viable, indicating their synthetic lethality (Figure 4A, left). Rpn10 is a proteasome regulatory particle (RP) subunit that maintains the structural integrity of the RP while also acting as a polyubiquitin receptor (Glickman et al., 1998; Tomko and Hochstrasser, 2011). Cells lacking *RPN10* are viable, but *rpn10Δ cdc48-3* double mutants were also synthetically lethal (Figure 4A, right). The synthetic lethality between *cdc48-3* and two mutants (*rpn4Δ* and *rpn10Δ*) that show compromised UPS function suggests that the *cdc48-3* mutation likely impairs UPS function as well. We next analyzed the genetic interaction between *cdc48-3* and *ubr2Δ* mutants. Ubr2 is an E3 ubiquitin ligase that targets Rpn4 for degradation; thus, *ubr2Δ* cells accumulate high levels of the Rpn4 protein, which increases the expression of proteasome subunits (Wang et al., 2004; Xie and Varshavsky, 2001). In clear contrast, we found that *UBR2* deletion partially rescued the growth defects of *cdc48-3*, *npl4-1*, and *ufd1-2* mutants at 34°C (Figure 4B). This is consistent with a previous finding that Rpn4 overexpression suppresses the growth defect of *cdc48-3* function (Chien and Chen, 2013). Together, these results indicate impaired UPS function in *cdc48* mutants.

The Accumulation of Ubiquitinated Proteins on Proteasomes Plays an Insignificant Role in the Growth Defect of *cdc48* Mutants

Previous studies showed increased accumulation of ubiquitinated proteins on proteasomes in *cdc48* mutants (Tsuchiya et al., 2017; Verma et al., 2011). This enhanced proteasome occupancy may compromise normal cellular protein turnover. Thus, we first confirmed the accumulation of ubiquitinated substrates on proteasomes by using a previously described protocol (Tsuchiya et al., 2017). WT and *cdc48-3* mutant cells expressing 3× FLAG-tagged Rpn11, a proteasome subunit, were grown at a semi-permissive temperature (34°C), and proteasomes were isolated by immunoprecipitating Rpn11. We noticed that the accumulation of ubiquitinated substrates on proteasomes in *cdc48-3* mutant cells was greater than that in WT cells (Figure 4C). Here, we used anti-ubiquitin immunoblotting of a 4% SDS-PAGE gel to detect ubiquitinated high-molecular-weight species. Using Htt103QP as a model misfolded protein, we also detected an increased association of Htt103QP with proteasomes in *cdc48-3* mutant cells (Figure S3), suggesting that Cdc48 deficiency leads to increased association of misfolded proteins with proteasomes. Because San1 and Ubr1 are primarily responsible for the ubiquitination of misfolded proteins, we examined whether their absence would decrease the association of misfolded proteins with proteasomes in the *cdc48-3* mutant. Not surprisingly, we found that the accumulation of ubiquitinated proteins on proteasomes in *cdc48-3* mutants was partially suppressed by *san1Δ ubr1Δ* (Figure S4). These results support the notion that Cdc48 deficiency increases the accumulation of ubiquitinated misfolded proteins on proteasomes, which is consistent with the previous observation (Tsuchiya et al., 2017).

It has been shown that the proteasome shuttling factors Dsk2 and Rad23 are responsible for the increased accumulation of ubiquitinated substrates on proteasomes in *cdc48-3* mutant cells (Tsuchiya et al., 2017). Our results confirmed Dsk2/Rad23-dependent proteasome accumulation of ubiquitinated proteins in *cdc48-3* mutant cells (Figure S5). Surprisingly, the *dsk2Δ rad23Δ* mutation did not suppress the temperature sensitivity of *cdc48-3* mutants but rather resulted in a more severe growth defect at both 25°C and 34°C (Figure 4D). Although more ubiquitinated substrates accumulate on proteasomes in *cdc48-3* mutant cells, this result indicates that this accumulation may play a minor role in the growth defect caused by Cdc48 deficiency. The synthetic growth defect of *cdc48-3 dsk2Δ rad23Δ* could be explained by the roles of Dsk2, Rad23, and Cdc48 in UPS-dependent protein degradation and suggests the source of misfolded protein toxicity lies upstream of the segregation of aggregates and delivery to the proteasome.

San1/Ubr1 Ubiquitin Ligases and the Cdc48 Complex Control Ubiquitin Homeostasis

We showed San1/Ubr1-dependent accumulation of ubiquitinated proteins in cells with dysfunctional $Cdc48^{Ufd1/Npl4}$ (Figures 3C and 3D). This accumulation may decrease free ubiquitin levels. If so, deletion of *SAN1* and *UBR1* may abolish this decrease. Thus, we incubated WT, *cdc48-3*, *npl4-1*, and *ufd1-2* mutant cells at 34°C for 5 h and then examined their free

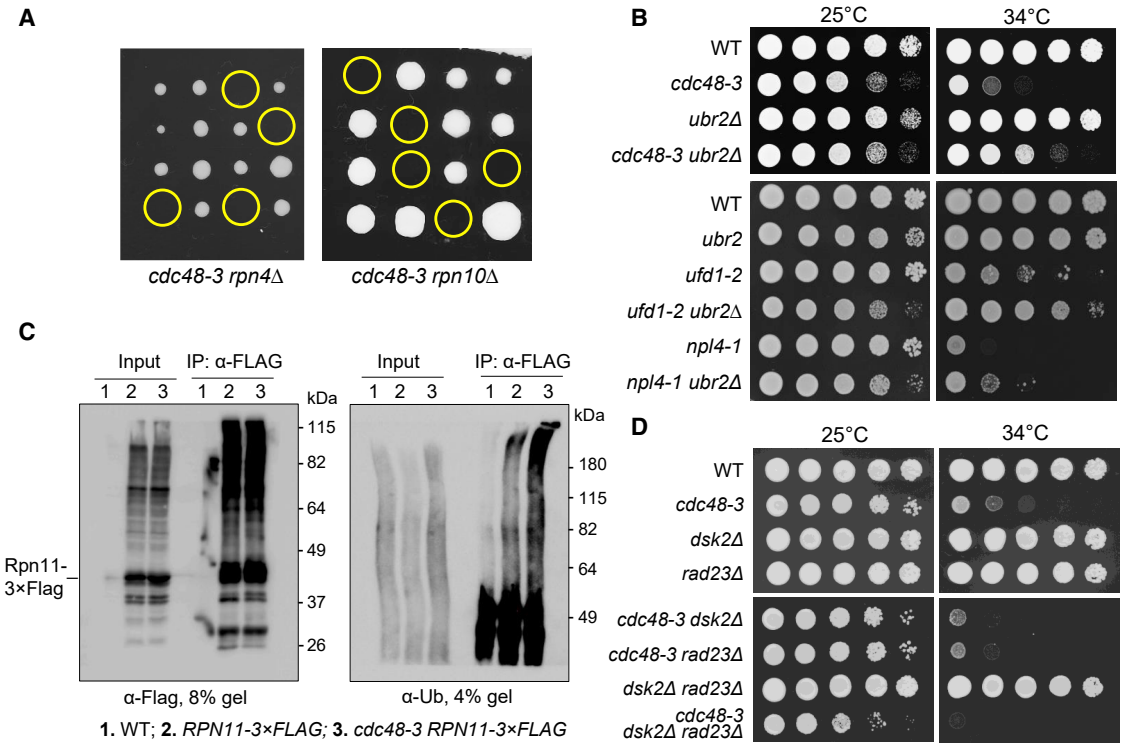

Figure 4. *cdc48* Mutants Show Compromised UPS Function

(A) The *cdc48-3* mutation is synthetically lethal with *rpn4Δ* and *rpn10Δ*. The *cdc48-3* mutant was crossed to *rpn4Δ* and *rpn10Δ* mutants to obtain diploid cells. The growth of the resultant spores at 25°C after tetrad dissection is shown. Yellow circles indicate spores of *cdc48-3 rpn4Δ* or *cdc48-3 rpn10Δ* double mutants.

(B) The temperature sensitivity of *cdc48-3*, *npl4-1*, and *ufd1-2* mutants is partially suppressed by *ubr2Δ*. Cells with the indicated genotypes were grown to saturation in YPD, 10-fold serially diluted, and spotted onto YPD plates. Cells were grown at 25°C and 34°C for 2 days. The yeast strains used in this experiment were WT (Y300), *cdc48-3* (MHY3512), *ubr2*Δ (3969-4-4), *cdc48-3 ubr2*Δ (3655-2-4), *npl4-1* (1126), *ufd1-2* (1122), *npl4-1 ubr2*Δ (3658-1-4), and *ufd1-2 ubr2*Δ (3659-1-2).

(C) The *cdc48-3* mutant cells show increased accumulation of ubiquitinated substrates on proteasomes. Log-phase cells of *pdr5Δ* (3589-1-4), *pdr5Δ RPN11-3* × *FLAG* (3592-4-4), and *pdr5Δ cdc48-3 RPN11-3* × *FLAG* (3592-5-2) grown in 25°C YPD were shifted to 34°C for 3 h. MG-132 was then added at 50 μM for 1 h to inhibit proteasome activity. The cells were then lysed, the Rpn11-3 × FLAG protein was immunoprecipitated using M2 anti-FLAG beads, and ubiquitinated proteins were detected using anti-Ub antibody. We used 4% SDS-PAGE to visualize high-molecular-weight ubiquitinated species (right panel).

(D) *dsk2*Δ *rad23*Δ mutation does not rescue the growth defect in *cdc48* mutants. Cells with indicated genotypes were grown in YPD to saturation, then 10-fold serially diluted, and spotted onto YPD plates. Cells were grown at 25°C or 34°C for 2 days. The strains used were WT (Y300), *cdc48-3* (MHY3512), *dsk2*Δ (YYW14), *rad23*Δ (3553-2-4), *cdc48-3 dsk2*Δ (3553-7-2), *cdc48-3 rad23*Δ (3553-10-3), *dsk2Δ rad23Δ* (3553-5-3), and *cdc48-3 dsk2*Δ *rad23*Δ (3553-3-2).

ubiquitin levels. Indeed, all three mutants exhibited a significant decrease of free ubiquitin compared to WT cells, and the difference was statistically significant. Remarkably, a *san1Δ ubr1Δ* mutation restored free ubiquitin levels in all of these mutants (Figure 5A). These results suggest that the accumulation of ubiquitinated protein species in $Cdc48^{Ufd1/Npl4}$ mutants decreases the free ubiquitin pool and that blocking misfolded protein ubiquitination by deleting *SAN1* and *UBR1* restores free ubiquitin levels.

We showed that *san1Δ ubr1Δ* mutants suppress the growth defect of $Cdc48^{Ufd1/Npl4}$ mutants at elevated temperatures (Figure 3). If this suppression is attributable to the restoration of free ubiquitin levels, high levels of ubiquitin expression should also suppress the growth defect in these mutants. Therefore, we introduced an empty vector or P_{GAL}*HA-Ub* (ubiquitin) plasmid into WT, *cdc48-3*, *npl4-1*, and *ufd1-2* cells. Ubiquitin overexpression partially rescued the temperature sensitivity of *cdc48-3* and *ufd1-2* mutants at 32°C and 34°C (Figure 5B). Although ubiquitin overexpression did not suppress the growth defect of the *npl4-1* mutant at 34°C, the overexpression did improve its growth at 25°C and 30°C (Figure 5C). We confirmed the induction of hemagglutinin (HA)-tagged ubiquitin in galactose medium (Figure S6A). In contrast to this result, a previous study showed that expression of monomeric ubiquitin from a high copy number plasmid (2μ) under a *GAP1* promoter was toxic to a *cdc48-3* mutant (Kimura et al., 2009). To clarify this discrepancy, WT and *cdc48-3* mutant cells were transformed with an empty vector or P_{ADH1}*RPS31(UBI3)* plasmid, which expresses a high level of yeast ubiquitin (*UBI3*) from a strong *ADH1* promotor (Lee et al., 2017). Although the suppression of the temperature sensitivity of *cdc48-3* by P_{ADH1}*RPS31* was not as clear as P_{GAL}*HA-Ub*, ubiquitin overexpression using this plasmid did not show toxicity to *cdc48-3* (Figure S6B).

If the function of Cdc48 is to promote ubiquitin homeostasis, decreased free ubiquitin levels would be expected to exacerbate the growth defect of *cdc48* mutants. However, deleting one of the ubiquitin encoding genes, *UBI4*, in *cdc48-3* mutants

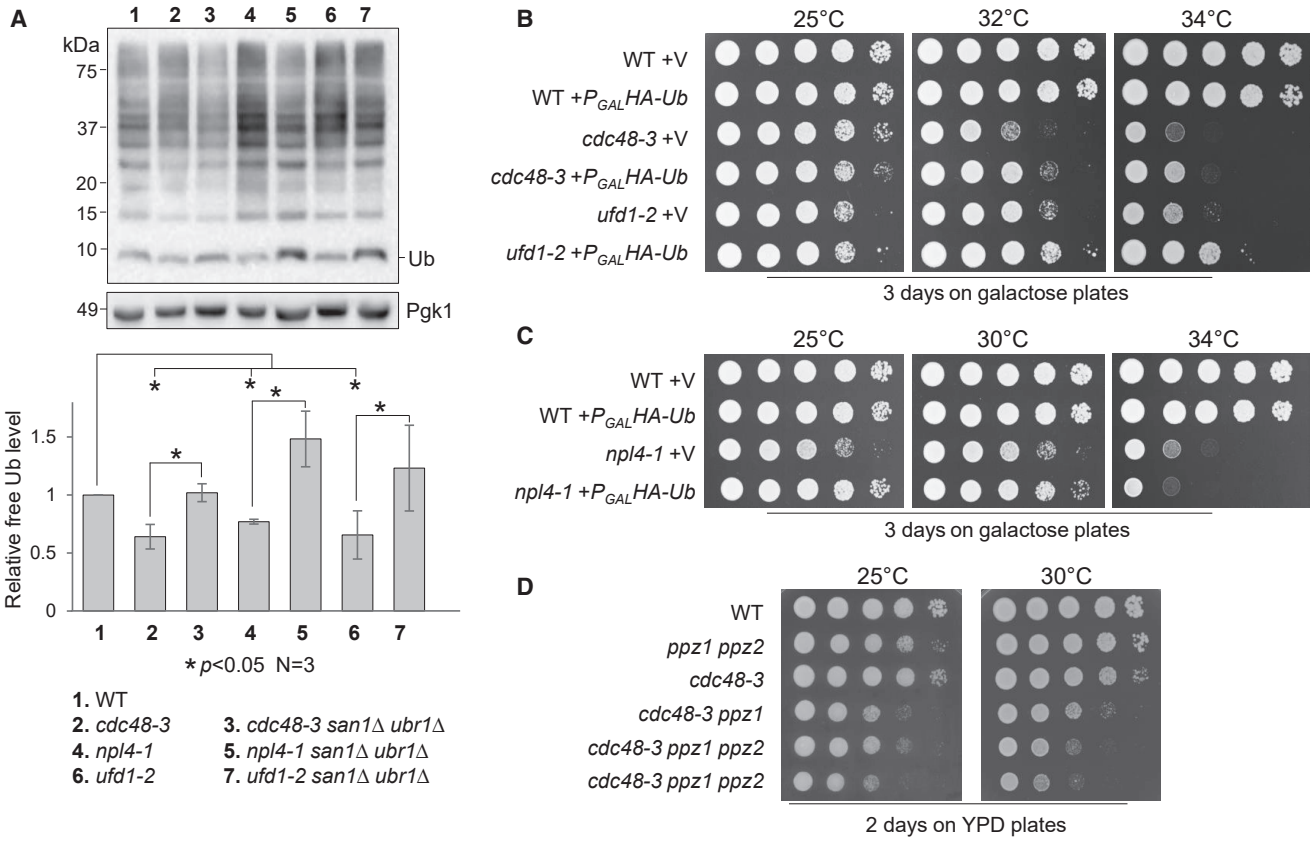

Figure 5. Disrupted Ubiquitin Homeostasis and the Growth Defect of *cdc48* Mutants

(A) Cdc48$^{Ufd1/Npl4}$ mutants show decreased free ubiquitin. Cells with the indicated genotypes were first grown in YPD at 25°C to mid-log phase and then shifted to 34°C for 5 h. Samples were prepared using Laemmli buffer (no lysis method used). Samples were resolved using Tricine-SDS-PAGE. Unconjugated (free) ubiquitin levels were detected using anti-Ub antibody. Pgk1, loading control. ImageJ was used to measure the intensity of mono-ubiquitin and Pgk1 bands. The ubiquitin/Pgk1 ratio represents the relative free ubiquitin level. The quantified result (mean ± SD) is from three independent experiments. *$p < 0.05$. Strains used in this experiment were WT (Y300), *cdc48-3* (MHY3512), *cdc48-3 san1Δ ubr1Δ* (3550-2-1), *npl4-1* (1126), *npl4-1 san1Δ ubr1Δ* (3555-5-1), *ufd1-2* (1122), and *ufd1-2 san1Δ ubr1Δ* (3556-3-3).

(B) Overexpression of ubiquitin partially rescues the temperature sensitivity of *cdc48-3* and *ufd1-2* mutants. WT (Y300), *cdc48-3* (MHY3512), and *ufd1-2* (1122) cells containing either *CEN-TRP1* control vector p1217 (V) or P_{GAL}*HA-Ub* (Ub) were grown to saturation in TRP (tryptophan) dropout medium containing raffinose, then 10-fold serially diluted, and spotted onto TRP dropout plates containing galactose. Cells were grown at 25°C, 32°C, and 34°C for 3 days.

(C) Overexpression of ubiquitin partially rescues the temperature sensitivity of *npl4-1*. WT (Y300) and *npl4-1* (1126) with vector and P_{GAL}*HA-Ub* plasmid were used for this experiment. The plates were incubated at 25°C, 30°C, and 34°C for 3 days.

(D) Deletion of ubiquitin kinases exacerbates the growth defect of *cdc48-3* mutants. Saturated WT, *ppz1Δ ppz2Δ* (PHY648), *cdc48-3* (MHY3512), *cdc48-3 ppz1Δ* (4023-1-1), and *cdc48-3 ppz1Δ ppz2Δ* (4023-2-4, 4023-8-4) cells were serially 10-fold diluted and spotted onto YPD plates. The plates were imaged after a 3-day incubation at 25°C and 30°C.

failed to cause a synthetic growth defect at the temperatures tested. The observation that the expression of the *UBI4* gene is only induced by stresses may explain this result (Finley et al., 1987). A recent study shows that Ppz1 and Ppz2 phosphorylate ubiquitin protein at Ser57, which stabilizes ubiquitin. Ubiquitin levels decrease in yeast cells lacking Ppz1 and Ppz2 (Lee et al., 2017). Strikingly, we found that deletion of either *PPZ1* alone or both *PPZ1* and *PPZ2* aggravated the growth defect of *cdc48-3* cells at both 25°C and 30°C (Figure 5D), indicating that *cdc48* mutant cells are sensitive to a reduced free ubiquitin pool. This result argues against the proteasome occupancy model, as decreased ubiquitin levels would decrease the delivery of ubiquitinated protein aggregates to the proteasome and thus would be expected to "unclog" the proteasome. Together, these results suggest that the Cdc48$^{Ufd1/Npl4}$ complex may drive ubiquitin recycling by disaggregating ubiquitinated protein aggregates. Furthermore, it suggests that a reduced free ubiquitin pool likely contributes to the growth defect in mutants with impaired Cdc48$^{Ufd1/Npl4}$ function.

Compromised UPS Function in *cdc48* Mutants and Ubiquitin Homeostasis

Our preceding results indicate compromised UPS activity and a ubiquitin homeostasis defect in *cdc48* mutant cells. The reduced free ubiquitin level in *cdc48* mutants may lead to compromised UPS function. To test this idea, we further verified compromised UPS activity in *cdc48-3* cells by measuring the degradation kinetics of Clb5, an S-phase cyclin. Clb5 shows ubiquitin-

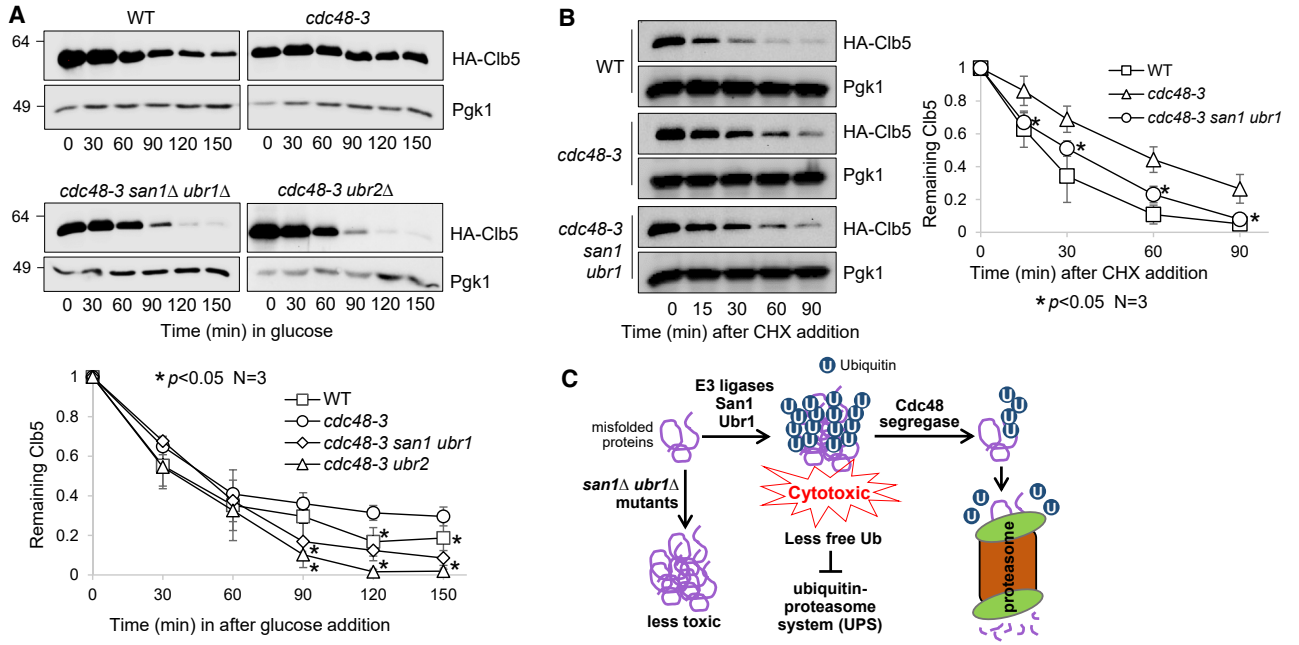

Figure 6. The Ubiquitination of Misfolded Proteins Compromises UPS Function in *cdc48* Mutants

(A) The *cdc48-3* mutant shows compromised degradation of S-phase cyclin Clb5, and this defect is suppressed by enhanced proteasome activity or decreased ubiquitination of misfolded proteins. WT (FY-13-1), *cdc48-3* (3504-3-2), *cdc48-3 san1Δ ubr1Δ* (3580-1-3), and *cdc48-3 ubr2Δ* (3660-1-4) cells containing P_{GAL}*HA-CLB5* were grown to mid-log phase in YPR (raffinose medium) at 25°C and then treated with α-factor for G_1 phase arrest for 2 h. Cells were shifted to 34°C for 30 min, and galactose was added for 1 h to induce HA-Clb5 overexpression. Glucose was then added to shut off HA-Clb5 expression. Cells were collected to determine HA-Clb5 protein levels. G_1 arrest was maintained throughout the experiment. Pgk1, loading control. The relative level of HA-Clb5 to Pgk1 was analyzed using ImageJ. The quantification shown at the bottom is the average of three independent experiments (mean ± SD). *p < 0.05.

(B) *san1Δ ubr1Δ* mutation alleviates the compromised degradation of endogenous Clb5 in *cdc48-3* mutant cells using CHX chase. WT (229-3-2), *cdc48-3* (3968-5-1), and *cdc48-3 san1Δ ubr1Δ* (3968-4-3) cells with HA-tagged *CLB5* in the chromosome locus were grown to mid-log phase in YPD at 25°C, and then the temperature was shifted to 34°C. After temperature shift for 30 min, CHX (200 μg/mL) was added to the medium, and cells were collected over time to examine the HA-Clb5 protein level using an anti-HA antibody. Pgk1, loading control. The experiment was repeated three times. The quantification results are represented as mean ± SD on the right panel. *p < 0.05.

(C) Working model. San1 and Ubr1 E3 ligases ubiquitinate misfolded proteins, which form aggregates. Cdc48-dependent disaggregation enables the degradation of misfolded proteins and ubiquitin recycling. Deletion of *SAN1* and *UBR1* overcomes the requirement for the Cdc48 complex in ubiquitin recycling.

dependent proteasomal degradation (Shirayama et al., 1999; Wang et al., 2001). We used a glucose shutoff assay to compare Clb5 stability in WT and *cdc48-3* mutant cells incubated at 34°C, as described for Htt103QP. To rule out any cell-cycle-related effects on protein degradation, the cells were arrested in G_1 phase for the entire experiment using the α-factor. After HA-Clb5 expression shutoff, *cdc48-3* cells showed a slower rate for Clb5 degradation than WT cells, as indicated by the significantly higher level of Clb5 in *cdc48-3* cells than WT cells after Clb5 expression was turned off for 120 and 150 min (Figure 6A), suggesting that functional Cdc48 is required for the efficient destruction of proteasomal substrates. We have shown that the temperature sensitivity of *cdc48-3* is suppressed either by a *ubr2*Δ mutant, which increases the expression of proteasome subunits, or by *san1Δ ubr1Δ* mutation, which decreases the ubiquitination of misfolded proteins. Strikingly, both *ubr2*Δ and *san1Δ ubr1Δ* mutations significantly suppressed the Clb5 degradation defect in *cdc48-3* cells (Figure 6A). As a segregase, Cdc48 may facilitate Clb5 degradation by separating cyclin Clb5 from cyclin-dependent kinase, but the suppression of the Clb5 degradation defect in *cdc48-3* cells by deletion of San1 and Ubr1 argues against this possibility. In addition, we used the cycloheximide chase method to assess the degradation kinetics of endogenous Clb5 in WT, *cdc48-3*, and *cdc48-3 san1*Δ *ubr1*Δ strains expressing *HA-CLB5*. Compromised Clb5 degradation was also observed in *cdc48-3* mutant cells after cycloheximide addition. A *san1Δ ubr1Δ* mutation suppressed the Clb5 degradation defect in *cdc48-3* mutant cells (Figure 6B). These results suggest that Cdc48 deficiency compromises proteasome-mediated protein degradation, and this UPS defect is likely caused by the accumulation of misfolded protein aggregates, which decreases the free ubiquitin pool.

DISCUSSION

This research provides novel insight into the nature of the cytotoxicity of misfolded proteins. Our results suggest that ubiquitination of misfolded proteins causes toxicity to cells at least in part by depleting free ubiquitin, thereby compromising UPS function. In response to proteotoxic stress, the Cdc48 complex alleviates the cytotoxicity by promoting the disaggregation of ubiquitinated protein aggregates and driving ubiquitin recycling.

Blocking misfolded protein ubiquitination in yeast cells by deleting E3 ligases San1 and Ubr1 decreases the cytotoxicity of misfolded proteins and reduces dependence on the $Cdc48^{Ufd1/Npl4}$ complex to combat proteotoxicity (Figure 6C).

Although the $Cdc48^{Ufd1/Npl4}$ complex has been shown to extract ubiquitinated substrates from membranes and macromolecular complexes (Blythe et al., 2017; Bodnar and Rapoport, 2017b; Twomey et al., 2019), it remains largely unknown how $Cdc48^{Ufd1/Npl4}$ acts in the proteotoxic stress response. Using Htt103QP as a model misfolded protein, we found compromised Htt103QP degradation and elevated accumulation of ubiquitinated Htt103QP in *cdc48-3* mutant cells. Furthermore, using an endogenous marker of protein aggregates, Hsp104-GFP, we also observed increased protein aggregation in cells with $Cdc48^{Ufd1/Npl4}$ deficiency. These results indicate the role of Cdc48 in segregating ubiquitinated protein aggregates, which likely facilitates protein degradation and ubiquitin recycling.

E3 ligases San1 and Ubr1 are responsible for the ubiquitination of misfolded proteins in budding yeast (Samant et al., 2018). One interesting observation is that deletion of San1 and Ubr1 suppresses the growth defect in cells with Cdc48 deficiency. Because deletion of these two ubiquitin ligases impairs ubiquitination of misfolded proteins, the accumulation of ubiquitinated proteins is likely a contributing factor to the growth defect in $Cdc48^{Ufd1/Npl4}$ mutants. Two avenues were explored for the reason why the accumulation of ubiquitinated proteins is toxic. First, the polyubiquitinated protein aggregates occupy proteasomes and compromise their function. Second, the accumulation of polyubiquitinated proteins decreases free ubiquitin levels, which impairs UPS function indirectly. Our results support the second possibility.

Our findings, combined with previous reports, indicate that dysfunctional Cdc48 results in the accumulation of polyubiquitinated substrates on proteasomes (Tsuchiya et al., 2017; Verma et al., 2011). The absence of proteasome shuttling factors Rad23 and Dsk2 abolishes this accumulation (Tsuchiya et al., 2017) but yields no suppression of the growth defect of *cdc48-3* cells. Although we cannot exclude the possibility that the occupancy of proteasomes by misfolded protein aggregates impairs UPS function, this may not be the major contribution to the growth defect in *cdc48*-3 cells. We have provided several lines of evidence indicating that polyubiquitinated protein aggregates act as a sponge to drain the free ubiquitin pool and impair UPS function. First, the absence of San1 and Ubr1 ubiquitin ligases reduces the accumulation of polyubiquitinated protein species in *cdc48*-3, *npl4-1*, and *ufd1*-2 mutants, while also partially suppressing their growth defects. Second, *san1*Δ *ubr1*Δ restores the efficiency of UPS-dependent degradation of cyclin Clb5 in *cdc48-3* mutant cells. Third, and importantly, ubiquitin overexpression suppresses the temperature sensitivity of $Cdc48^{Ufd1/Npl4}$ complex mutants, but a lower free ubiquitin level caused by *ppz1Δ ppz2Δ* exacerbates the growth defect of *cdc48-3* mutants. Together, our data suggest a new mechanism for how misfolded proteins impose cytotoxicity. The ubiquitination of misfolded proteins appears to be a double-edged sword. Cells target misfolded proteins for degradation through their ubiquitination; however, under certain conditions, this drains free ubiquitin and impairs UPS function. Given the high abundance of the Cdc48 protein (Baek et al., 2013), cells are well equipped to combat spontaneous protein misfolding and aggregation, but upon Cdc48 inactivation, the accumulation of polyubiquitinated protein aggregates poses a greater risk to cell health.

Overall, our findings highlight that ubiquitination of misfolded proteins can cause cytotoxicity if not degraded in a timely manner, at least in part due to the decrease of the free ubiquitin pool. Moreover, our results suggest that the $Cdc48^{Ufd1/Npl4}$ complex not only facilitates proteasomal degradation of misfolded proteins but also indirectly stimulates ubiquitin recycling. In addition, the absence of two ubiquitin ligases, San1 and Ubr1, known to target misfolded proteins results in a decrease in the toxicity of misfolded proteins. Our data support a novel mechanism by which misfolded proteins cause cytotoxicity and highlight the important roles of the $Cdc48^{Ufd1/Npl4}$ segregase and ubiquitin ligases in ubiquitin homeostasis (Figure 6C).

The $Cdc48^{Ufd1/Npl4}$ complex is conserved from yeast to humans, indicating that human cells likely use the same mechanism to combat the cytotoxicity of misfolded proteins. Mutations in the human Cdc48 segregase p97/VCP are associated with inclusion body myopathy with Paget disease of bone (Watts et al., 2004). Additionally, aneuploid cancer cells show increased proteotoxic stress due to the synthesis of unnecessary proteins, which results in hypersensitivity to inhibitors of Cdc48/p97 (Chapman et al., 2015; Luo et al., 2009). Furthermore, recent research indicates the anticancer activity of the alcohol-abuse drug disulfiram, which targets Cdc48 cofactor Npl4 (Skrott et al., 2017). Therefore, our research provides a new angle to understand the function of the Cdc48 complex in response to proteotoxic stress.

STAR★METHODS

Detailed methods are provided in the online version of this paper and include the following:

- KEY RESOURCES TABLE
- RESOURCE AVAILABILITY
  - Lead Contact
  - Materials Availability
  - Data and Code Availability
- EXPERIMENTAL MODEL AND SUBJECT DETAILS
- METHOD DETAILS
  - Western Blotting
  - Ubiquitination of Htt103QP
  - The interaction of ubiquitinated substrates with proteasomes
  - Monitoring degradation of Htt103QP
  - Clb5 degradation kinetics
  - Free ubiquitin detection
  - Fluorescence imaging
- QUANTIFICATION AND STATISTICAL ANALYSIS

SUPPLEMENTAL INFORMATION

Supplemental Information can be found online at https://doi.org/10.1016/j.celrep.2020.107898.

ACKNOWLEDGMENTS

We sincerely thank Drs. Timothy Megraw, Yi Zhou, and Hong-Guo Yu and the yeast community at Florida State University (FSU) for comments and suggestions for this project. We thank Drs. Rey-Huei Chen, Mark Hochstrasser, and Jason MacGurn for yeast strains and plasmids. We highly appreciate the careful editing of the manuscript by Dr. Terra Bradley. We thank Dr. Wen Li from Department of Psychology, at FSU, for her advice on statistical analysis. We thank the FSU Biology Core Facility for DNA sequencing. This work was supported by a CRC planning grant from FSU, partly by R01GM121786 from National Institute of Health (USA) to Y.W. and partly by R01GM118600 to R.J.T.

AUTHOR CONTRIBUTIONS

Conceptualization, Y.W., R.H., and R.J.T.; Methodology, R.H., M.-H.K., R.J.T., and Y.W.; Investigation, R.H., M.-H.K., D.S., L.A.H., A.H., and Y.W.; Writing – Original Draft, R.H. and Y.W.; Writing – Review & Editing, R.H., R.J.T., and Y.W.; Funding Acquisition, R.J.T. and Y.W.; Supervision, R.J.T. and Y.W.

DECLARATION OF INTERESTS

There are no competing interests.

Received: August 7, 2019
Revised: May 4, 2020
Accepted: June 22, 2020
Published: July 14, 2020

REFERENCES

Aguado, A., Fernández-Higuero, J.A., Moro, F., and Muga, A. (2015). Chaperone-assisted protein aggregate reactivation: Different solutions for the same problem. Arch. Biochem. Biophys. *580*, 121–134.

Baek, G.H., Cheng, H., Choe, V., Bao, X., Shao, J., Luo, S., and Rao, H. (2013). Cdc48: a swiss army knife of cell biology. J. Amino Acids *2013*, 183421.

Bersuker, K., Brandeis, M., and Kopito, R.R. (2016). Protein misfolding specifies recruitment to cytoplasmic inclusion bodies. J. Cell Biol. *213*, 229–241.

Blythe, E.E., Olson, K.C., Chau, V., and Deshaies, R.J. (2017). Ubiquitin- and ATP-dependent unfoldase activity of P97/VCP·NPLOC4·UFD1L is enhanced by a mutation that causes multisystem proteinopathy. Proc. Natl. Acad. Sci. USA *114*, E4380–E4388.

Bodnar, N., and Rapoport, T. (2017a). Toward an understanding of the Cdc48/p97 ATPase. F1000Res. *6*, 1318.

Bodnar, N.O., and Rapoport, T.A. (2017b). Molecular Mechanism of Substrate Processing by the Cdc48 ATPase Complex. Cell *169*, 722–735.e729.

Bodnar, N.O., Kim, K.H., Ji, Z., Wales, T.E., Svetlov, V., Nudler, E., Engen, J.R., Walz, T., and Rapoport, T.A. (2018). Structure of the Cdc48 ATPase with its ubiquitin-binding cofactor Ufd1-Npl4. Nat. Struct. Mol. Biol. *25*, 616–622.

Chapman, E., Maksim, N., de la Cruz, F., and La Clair, J.J. (2015). Inhibitors of the AAA+ chaperone p97. Molecules *20*, 3027–3049.

Chien, C.Y., and Chen, R.H. (2013). Cdc48 chaperone and adaptor Ubx4 distribute the proteasome in the nucleus for anaphase proteolysis. J. Biol. Chem. *288*, 37180–37191.

Chuang, K.H., Liang, F., Higgins, R., and Wang, Y. (2016). Ubiquilin/Dsk2 promotes inclusion body formation and vacuole (lysosome)-mediated disposal of mutated huntingtin. Mol. Biol. Cell *27*, 2025–2036.

Dasgupta, A., Ramsey, K.L., Smith, J.S., and Auble, D.T. (2004). Sir Antagonist 1 (San1) is a ubiquitin ligase. J. Biol. Chem. *279*, 26830–26838.

de Oliveira, G.A., Rangel, L.P., Costa, D.C., and Silva, J.L. (2015). Misfolding, Aggregation, and Disordered Segments in c-Abl and p53 in Human Cancer. Front. Oncol. *5*, 97.

Dehay, B., and Bertolotti, A. (2006). Critical role of the proline-rich region in Huntingtin for aggregation and cytotoxicity in yeast. J. Biol. Chem. *281*, 35608–35615.

Eisele, F., and Wolf, D.H. (2008). Degradation of misfolded protein in the cytoplasm is mediated by the ubiquitin ligase Ubr1. FEBS Lett. *582*, 4143–4146.

Fang, N.N., Ng, A.H., Measday, V., and Mayor, T. (2011). Hul5 HECT ubiquitin ligase plays a major role in the ubiquitylation and turnover of cytosolic misfolded proteins. Nat. Cell Biol. *13*, 1344–1352.

Finley, D., Ozkaynak, E., and Varshavsky, A. (1987). The yeast polyubiquitin gene is essential for resistance to high temperatures, starvation, and other stresses. Cell *48*, 1035–1046.

Finley, D., Ulrich, H.D., Sommer, T., and Kaiser, P. (2012). The ubiquitin-proteasome system of Saccharomyces cerevisiae. Genetics *192*, 319–360.

Gardner, R.G., Nelson, Z.W., and Gottschling, D.E. (2005). Degradation-mediated protein quality control in the nucleus. Cell *120*, 803–815.

Ghosh, D.K., Roy, A., and Ranjan, A. (2018). The ATPase VCP/p97 functions as a disaggregase against toxic Huntingtin-exon1 aggregates. FEBS Lett. *592*, 2680–2692.

Glickman, M.H., Rubin, D.M., Coux, O., Wefes, I., Pfeifer, G., Cjeka, Z., Baumeister, W., Fried, V.A., and Finley, D. (1998). A subcomplex of the proteasome regulatory particle required for ubiquitin-conjugate degradation and related to the COP9-signalosome and eIF3. Cell *94*, 615–623.

Hartl, F.U., Bracher, A., and Hayer-Hartl, M. (2011). Molecular chaperones in protein folding and proteostasis. Nature *475*, 324–332.

Heck, J.W., Cheung, S.K., and Hampton, R.Y. (2010). Cytoplasmic protein quality control degradation mediated by parallel actions of the E3 ubiquitin ligases Ubr1 and San1. Proc. Natl. Acad. Sci. USA *107*, 1106–1111.

Higgins, R., Kabbaj, M.H., Hatcher, A., and Wang, Y. (2018). The absence of specific yeast heat-shock proteins leads to abnormal aggregation and compromised autophagic clearance of mutant Huntingtin proteins. PLoS One *13*, e0191490.

Hipp, M.S., Patel, C.N., Bersuker, K., Riley, B.E., Kaiser, S.E., Shaler, T.A., Brandeis, M., and Kopito, R.R. (2012). Indirect inhibition of 26S proteasome activity in a cellular model of Huntington's disease. J. Cell Biol. *196*, 573–587.

Imamura, S., Yabu, T., and Yamashita, M. (2012). Protective role of cell division cycle 48 (CDC48) protein against neurodegeneration via ubiquitin-proteasome system dysfunction during zebrafish development. J. Biol. Chem. *287*, 23047–23056.

Jacobson, T., Navarrete, C., Sharma, S.K., Sideri, T.C., Ibstedt, S., Priya, S., Grant, C.M., Christen, P., Goloubinoff, P., and Tamás, M.J. (2012). Arsenite interferes with protein folding and triggers formation of protein aggregates in yeast. J. Cell Sci. *125*, 5073–5083.

Kimura, Y., Yashiroda, H., Kudo, T., Koitabashi, S., Murata, S., Kakizuka, A., and Tanaka, K. (2009). An inhibitor of a deubiquitinating enzyme regulates ubiquitin homeostasis. Cell *137*, 549–559.

Knowles, T.P., Vendruscolo, M., and Dobson, C.M. (2014). The amyloid state and its association with protein misfolding diseases. Nat. Rev. Mol. Cell Biol. *15*, 384–396.

Komander, D., Clague, M.J., and Urbé, S. (2009). Breaking the chains: structure and function of the deubiquitinases. Nat. Rev. Mol. Cell Biol. *10*, 550–563.

Krobitsch, S., and Lindquist, S. (2000). Aggregation of huntingtin in yeast varies with the length of the polyglutamine expansion and the expression of chaperone proteins. Proc. Natl. Acad. Sci. USA *97*, 1589–1594.

Lee, S., Tumolo, J.M., Ehlinger, A.C., Jernigan, K.K., Qualls-Histed, S.J., Hsu, P.C., McDonald, W.H., Chazin, W.J., and MacGurn, J.A. (2017). Ubiquitin turnover and endocytic trafficking in yeast are regulated by Ser57 phosphorylation of ubiquitin. eLife *6*, e29176.

Leitman, J., Ulrich Hartl, F., and Lederkremer, G.Z. (2013). Soluble forms of polyQ-expanded huntingtin rather than large aggregates cause endoplasmic reticulum stress. Nat. Commun. *4*, 2753.

Liu, C., Liu, W., Ye, Y., and Li, W. (2017). Ufd2p synthesizes branched ubiquitin chains to promote the degradation of substrates modified with atypical chains. Nat. Commun. *8*, 14274.

Longtine, M.S., McKenzie, A., III, Demarini, D.J., Shah, N.G., Wach, A., Brachat, A., Philippsen, P., and Pringle, J.R. (1998). Additional modules for

versatile and economical PCR-based gene deletion and modification in Saccharomyces cerevisiae. Yeast *14*, 953–961.

Lu, K., Psakhye, I., and Jentsch, S. (2014). Autophagic clearance of polyQ proteins mediated by ubiquitin-Atg8 adaptors of the conserved CUET protein family. Cell *158*, 549–563.

Luo, J., Solimini, N.L., and Elledge, S.J. (2009). Principles of cancer therapy: oncogene and non-oncogene addiction. Cell *136*, 823–837.

Miller, S.B., Mogk, A., and Bukau, B. (2015). Spatially organized aggregation of misfolded proteins as cellular stress defense strategy. J. Mol. Biol. *427*, 1564–1574.

Mogk, A., Bukau, B., and Kampinga, H.H. (2018). Cellular Handling of Protein Aggregates by Disaggregation Machines. Mol. Cell *69*, 214–226.

Mukherjee, A., Morales-Scheihing, D., Butler, P.C., and Soto, C. (2015). Type 2 diabetes as a protein misfolding disease. Trends Mol. Med. *21*, 439–449.

Ogen-Shtern, N., Ben David, T., and Lederkremer, G.Z. (2016). Protein aggregation and ER stress. Brain Res. *1648*, 658–666.

Olszewski, M.M., Williams, C., Dong, K.C., and Martin, A. (2019). The Cdc48 unfoldase prepares well-folded protein substrates for degradation by the 26S proteasome. Commun. Biol. *2*, 29.

Ravid, T., and Hochstrasser, M. (2007). Autoregulation of an E2 enzyme by ubiquitin-chain assembly on its catalytic residue. Nat. Cell Biol. *9*, 422–427.

Reyes-Turcu, F.E., Ventii, K.H., and Wilkinson, K.D. (2009). Regulation and cellular roles of ubiquitin-specific deubiquitinating enzymes. Annu. Rev. Biochem. *78*, 363–397.

Rosenbaum, J.C., Fredrickson, E.K., Oeser, M.L., Garrett-Engele, C.M., Locke, M.N., Richardson, L.A., Nelson, Z.W., Hetrick, E.D., Milac, T.I., Gottschling, D.E., and Gardner, R.G. (2011). Disorder targets misorder in nuclear quality control degradation: a disordered ubiquitin ligase directly recognizes its misfolded substrates. Mol. Cell *41*, 93–106.

Samant, R.S., Livingston, C.M., Sontag, E.M., and Frydman, J. (2018). Distinct proteostasis circuits cooperate in nuclear and cytoplasmic protein quality control. Nature *563*, 407–411.

Shirayama, M., Tóth, A., Gálová, M., and Nasmyth, K. (1999). APC(Cdc20) promotes exit from mitosis by destroying the anaphase inhibitor Pds1 and cyclin Clb5. Nature *402*, 203–207.

Skrott, Z., Mistrik, M., Andersen, K.K., Friis, S., Majera, D., Gursky, J., Ozdian, T., Bartkova, J., Turi, Z., Moudry, P., et al. (2017). Alcohol-abuse drug disulfiram targets cancer via p97 segregase adaptor NPL4. Nature *552*, 194–199.

Soto, C. (2003). Unfolding the role of protein misfolding in neurodegenerative diseases. Nat. Rev. Neurosci. *4*, 49–60.

Swaminathan, S., Amerik, A.Y., and Hochstrasser, M. (1999). The Doa4 deubiquitinating enzyme is required for ubiquitin homeostasis in yeast. Mol. Biol. Cell *10*, 2583–2594.

Tomko, R.J., Jr., and Hochstrasser, M. (2011). Incorporation of the Rpn12 subunit couples completion of proteasome regulatory particle lid assembly to lid-base joining. Mol. Cell *44*, 907–917.

Tsuchiya, H., Ohtake, F., Arai, N., Kaiho, A., Yasuda, S., Tanaka, K., and Saeki, Y. (2017). In Vivo Ubiquitin Linkage-type Analysis Reveals that the Cdc48-Rad23/Dsk2 Axis Contributes to K48-Linked Chain Specificity of the Proteasome. Mol. Cell *66*, 488–502.e487.

Twomey, E.C., Ji, Z., Wales, T.E., Bodnar, N.O., Ficarro, S.B., Marto, J.A., Engen, J.R., and Rapoport, T.A. (2019). Substrate processing by the Cdc48 ATPase complex is initiated by ubiquitin unfolding. Science *365*, eaax1033.

Tyedmers, J., Mogk, A., and Bukau, B. (2010). Cellular strategies for controlling protein aggregation. Nat. Rev. Mol. Cell Biol. *11*, 777–788.

Verma, R., Oania, R., Fang, R., Smith, G.T., and Deshaies, R.J. (2011). Cdc48/p97 mediates UV-dependent turnover of RNA Pol II. Mol. Cell *41*, 82–92.

Wang, H., Liu, D., Wang, Y., Qin, J., and Elledge, S.J. (2001). Pds1 phosphorylation in response to DNA damage is essential for its DNA damage checkpoint function. Genes Dev. *15*, 1361–1372.

Wang, L., Mao, X., Ju, D., and Xie, Y. (2004). Rpn4 is a physiological substrate of the Ubr2 ubiquitin ligase. J. Biol. Chem. *279*, 55218–55223.

Wang, Y., Meriin, A.B., Zaarur, N., Romanova, N.V., Chernoff, Y.O., Costello, C.E., and Sherman, M.Y. (2009). Abnormal proteins can form aggresome in yeast: aggresome-targeting signals and components of the machinery. FASEB J. *23*, 451–463.

Watts, G.D., Wymer, J., Kovach, M.J., Mehta, S.G., Mumm, S., Darvish, D., Pestronk, A., Whyte, M.P., and Kimonis, V.E. (2004). Inclusion body myopathy associated with Paget disease of bone and frontotemporal dementia is caused by mutant valosin-containing protein. Nat. Genet. *36*, 377–381.

Xie, Y., and Varshavsky, A. (2001). RPN4 is a ligand, substrate, and transcriptional regulator of the 26S proteasome: a negative feedback circuit. Proc. Natl. Acad. Sci. USA *98*, 3056–3061.

Yang, H., and Hu, H.Y. (2016). Sequestration of cellular interacting partners by protein aggregates: implication in a loss-of-function pathology. FEBS J. *283*, 3705–3717.

Yang, J., Hao, X., Cao, X., Liu, B., and Nyström, T. (2016). Spatial sequestration and detoxification of Huntingtin by the ribosome quality control complex. eLife *5*, e11792.

Ye, Y., Tang, W.K., Zhang, T., and Xia, D. (2017). A Mighty "Protein Extractor" of the Cell: Structure and Function of the p97/CDC48 ATPase. Front. Mol. Biosci. *4*, 39.

STAR★METHODS

KEY RESOURCES TABLE

REAGENT or RESOURCE	SOURCE	IDENTIFIER
Antibodies		
Mouse monoclonal anti-Flag	Sigma-Aldrich	Cat# F3165; RRID:AB_259529
Mouse monoclonal anti-Ubiquitin (P4D1)	Santa Cruz	Cat# Sc-8017; RRID:AB_2762364
Mouse monoclonal anti-Pgk1	Invitrogen	Cat# 459250; RRID:AB_2532235
Mouse monoclonal anti-HA	Biolegend	Cat# 901515; RRID:AB_2565334
Mouse anti-Flag M2 (agarose beads) affinity gel	Sigma	Cat# A2220; RRID:AB_10063035
Mouse anti-GFP antibody	Santa Cruz	Cat# Sc-9966; RRID:AB_627235
Secondary anti-mouse IgG HRP-linked antibody	Cell signaling	Cat# 7076; RRID:AB_330924
Chemicals, Peptides, and Recombinant Proteins		
MG132	Abcam	Ab141003
Protease inhibitor cocktail set III	Millipore-Calbiochem	539136
Deubiquitinase inhibitor N-ethylmaleimide	Sigma	E3876
Cycloheximide	Enzo Life Sciences	ALX380-269 G001
ECL	PerkinElmer	NEL 104001
Experimental Models: Organisms/Strains		
S. cerevisiae: strain background W303; see Table S1	This paper	N/A
Oligonucleotides		
SAN1 deletion forward primer ACTATAGATAGAAATTATTTAGCATTTCAGG ATAGTTCGTCGGATCCCCGGGTTAATTAA	This paper	N/A
SAN1 deletion reverse primer TGGATGACTGCCAATAGGACATATTTTCA TATTAACATACGAATTCGAGCTCGTTTAAAC	This paper	N/A
UBR1 deletion forward primer GTCCCTAATCTTTACAGGTCACACAAATT ACATAGAACATCGGATCCCCGGGTTAATTAA	This paper	N/A
UBR1 deletion reverse primer GTCAATCGACGCGCAAATGTTTAATAATGTAT AAGTTTTTGAATTCGAGCTCGTTTAAAC	This paper	N/A
HTA1-mApple forward primer AAAGAAGTCTGCCAAGGCTACCAAGGCTTC TCAAGAATTAGCGGCCGCTCTAGAACTAGTGG	This paper	N/A
HTA1-mApple reverse primer TTTAGTTCCTTCCGCCTTCTTTAAAATACCTGAA CCGATCCCCCCTCGAGGTCGACGGTATCG	This paper	N/A
Software and Algorithms		
ImageJ	National Institutes of Health	https://imagej.nih.gov/ij/

RESOURCE AVAILABILITY

Lead Contact

Further information and requests for resources and reagents should be directed to and will be fulfilled by the Lead Contact, Yanchang Wang (yanchang.wang@med.fsu.edu).

Materials Availability

All of the yeast strains and plasmids generated by this work will be available upon request.

Data and Code Availability

This study did not generate any unique datasets or code.

EXPERIMENTAL MODEL AND SUBJECT DETAILS

Yeast strains used in this study are of the W303 background. The relevant genotypes of the strains used in this study are listed in Table S2. Gene deletions and GFP tagging of *HSP104* were performed using a PCR-based method (Longtine et al., 1998). The P_{GAL}-*FLAG-Htt103QP-GFP* plasmid was originally from the Lindquist laboratory (Krobitsch and Lindquist, 2000). Manipulation of this plasmid and the construction of the p1217/P_{GAL}*HA-Ub* plasmid were previously described (Higgins et al., 2018). Yeast extract/peptone media supplied with raffinose (YPR), galactose (YPG), or glucose (YPD) were used for the growth of yeast strains, except for those carrying centromeric plasmids, in which case synthetic dropout medium was used.

METHOD DETAILS

Western Blotting

Unless otherwise noted, protein samples were prepared using an alkaline method and resolved by 8% SDS–PAGE. The resources of the antibodies used in this study are listed in the above table. After ECL, the western blot membranes were imaged using Bio-Rad ChemiDoc.

Ubiquitination of Htt103QP

The protocol was adapted from a previous publication (Higgins et al., 2018). Briefly, cells containing P_{GAL}*FLAG-Htt103QP-GFP* were grown in YPR (raffinose medium) to OD_{600} = 0.4. Galactose was then added to the medium to the final concentration of 2% to induce FLAG-Htt103QP-GFP expression for 3 hours. Ten mL of cells were harvested by centrifugation at 10,000 rpm for 5 minutes. Cells were washed once with water and resuspended in RIPA buffer (50 mM Tris-HCl pH 7.5, 150 mM NaCl, 5 mM EDTA, 0.05% Tween-20) along with sodium azide and protease inhibitor cocktail. Samples were frozen in liquid nitrogen and subsequently crushed using a freezer mill. Samples were then thawed on ice in the presence of 20 mM deubiquitinase inhibitor *N*-ethylmaleimide. After centrifugation at 15,000 rpm for 20 minutes at 4°C, the supernatant was collected and centrifuged again at 15,000 rpm for 20 minutes at 4°C. Input sample was taken prior to the addition of M2 FLAG agarose beads to immunoprecipitate FLAG-Htt103QP-GFP. Beads were washed three times, resuspended in Laemmli buffer, and boiled for 5 minutes. Western blotting was performed using anti-FLAG, anti-Ub, and anti-Pgk1 antibodies.

The interaction of ubiquitinated substrates with proteasomes

We used a previous protocol with minor modifications to detect the interaction of ubiquitinated substrates with proteasomes (Tsuchiya et al., 2017). All strains used in these experiments were in the *pdr5Δ* background, which allows efficient proteasome inhibition by the proteasome inhibitor MG-132 (Ravid and Hochstrasser, 2007). Briefly, cells were grown in 50 mL YPD (glucose medium) at 25°C to OD_{600} = 0.4, followed by a temperature shift to 34°C for 3 hours. MG-132 (50 μM) was added for one additional hour at 34°C. Cells were then harvested and resuspended in 10 mL YPD containing 1% of paraformaldehyde for 10 minutes. Glycine was then added at 250 mM to quench the paraformaldehyde. Cells were harvested, resuspended in 200 μl lysis buffer, and lysed by a bead beater. To the lysate, 200 μl of lysis buffer containing 2% Triton X-100 was added and samples were incubated on ice for 30 minutes. The samples were centrifuged at 15,000 rpm for 10 minutes. We removed 25 μl of supernatant as an input, and M2 anti-FLAG agarose beads were added to the remaining supernatant to immunoprecipitate Rpn11-3 × FLAG. The beads were washed three times with lysis buffer containing 1% Triton X-100. Beads were resuspended in NuPAGE 1 × SDS loading buffer (Invitrogen) and incubated at 65°C for 10 minutes. Samples were resolved using SDS-PAGE.

Monitoring degradation of Htt103QP

The degradation of Htt103QP was performed using a shut-off assay as described previously (Chuang et al., 2016; Higgins et al., 2018). Briefly, the expression of FLAG-Htt103QP-GFP was induced in YPG (galactose medium) for 1 hour, then glucose was added and the protein levels of Htt103QP were determined by western blotting using an anti-FLAG antibody.

The degradation of Htt103QP was also performed with cycloheximide chase assay. Cells with indicated genotypes were grown to mid-log phase. After Htt103QP expression was induced in YPG for 30 minutes, cycloheximide was added to the medium at the final concentration of 200 μg/mL. Cells were collected over time to measure Htt103QP protein levels.

Clb5 degradation kinetics

Cells containing an integrated P_{GAL}*HA-CLB5* plasmid were grown in YPR (raffinose medium) to mid-log phase at 25°C. To arrest cells in G_1 phase, we added α-factor (1 μg/mL) to cell cultures for 2 hours at 25°C, followed by a temperature shift to 34°C for 30 minutes. Galactose (2%) was added to induce HA-Clb5 overexpression for 1 hour, and then glucose (2%) was added to shut off expression. G_1 arrest was maintained throughout the entire experiment by adding α-factor at 1-hour intervals. Samples were prepared using the alkaline method, resuspended in Laemmli buffer, and boiled for 5 minutes. HA-Clb5 was detected using an anti-HA antibody.

Cycloheximide chase was also used to determine the degradation kinetics of endogenous Clb5 protein. Yeast strains expressing *CLB5-HA* from the endogenous promotor were grown to mid-log phase and cycloheximide was added to the medium to the final concentration of 200 μg/mL. Cells were collected over time to prepare protein samples as above. The protein level of Clb5 was determined by western blotting with anti-HA antibody.

Free ubiquitin detection

Yeast cells were inoculated into 5 mL of YPD (glucose medium) and incubated overnight at 25°C. The cultures were diluted to an OD_{600} of 0.1 in 5 mL of fresh YPD and incubated at 25°C for 90 minutes, then transferred to 34°C for 5 hours. The cells were harvested by centrifugation at 10,000 rpm for 1 minute. The resulting pellets were resuspended in 1 × Laemmli loading buffer and boiled at 95°C for 5 minutes. Samples were separated using 12% SDS-PAGE with Tris-Tricine running buffer. The gel was electrophoresed at 80 V for 15 minutes and then switched to 100 V until the dye front escaped. Gels were transferred to PVDF membranes (EMD Millipore) at 100 V for 1 hour at 4°C and immunoblotted with antibodies against ubiquitin and Pgk1. Band intensities were quantified using ImageJ, and the ubiquitin/Pgk1 ratio represents ubiquitin level.

Fluorescence imaging

Fluorescence imaging analysis was performed using an EVOS microscope (Thermo Fisher Scientific, Waltham, MA). For all imaging analysis, yeast cells were fixed in 4% paraformaldehyde for 5 minutes and then resuspended in 1 × PBS buffer.

QUANTIFICATION AND STATISTICAL ANALYSIS

To determine differences in protein degradation kinetics and the level of protein ubiquitination in different yeast strains, we used ImageJ to acquire the intensity of each protein band from western blotting images. Then the protein levels were normalized by determining the ratio to loading control, Pgk1. Normalized protein levels from three repeats were used to calculate the mean and standard deviation (SD). The Wilcoxon rank sum test was used to determine *p* values. Statistically significance was inferred when $p < 0.05$ (*).

To compare cluster formation of Hsp104-GFP (Figure 2C) or Htt103QP-GFP (Figure S2) clusters in WT and mutant cells, more than 100 cells were counted for each sample at a given time point. Cells with or without visible GFP clusters (Figure 2C) and the number of GFP foci (Figure S2) were counted and the experiments were repeated three times. We performed a two-way ANOVA on each dataset, and calculated the statistical significance of the differences between genotypes at each time point. The significance was corrected for multiple comparisons using Tukey's multiple comparisons test. We considered values significantly different if $p < 0.05$.

Cell Reports, Volume *32*

Supplemental Information

The Cdc48 Complex Alleviates the Cytotoxicity of Misfolded Proteins by Regulating Ubiquitin Homeostasis

Ryan Higgins, Marie-Helene Kabbaj, Delaney Sherwin, Lauren A. Howell, Alexa Hatcher, Robert J. Tomko Jr., and Yanchang Wang

SUPPLEMENTAL INFORMATION

Figure S1 (related to Figure 1). The proline-rich region in Huntingtin affects its aggregation and degradation. **A.** Cellular localization of Htt103QP-GFP and Htt103QΔP-GFP in yeast cells. Yeast cells with *P_{GAL}FLAG-Htt103QP-GFP* (3419-1-1) and *P_{GAL}FLAG-Htt103QΔP-GFP* (YYW313-1) were grown in raffinose medium to mid-log phase at 30°C. Galactose (final concentration 2%) was added and cell images were taken after a 6-hour incubation in galactose medium. The GFP signal is shown. Scale bar, 5μm. **B.** The degradation kinetics of Htt103QP and Htt103QΔP. The above yeast strains were grown in raffinose medium to mid-log phase. Galactose (final concentration 2%) was added for 1 hour to induce Htt103QP and Htt103QΔP expression, followed by addition of glucose to shut off the induction. Protein samples were prepared over time; Htt103QP and Htt103QΔP protein levels were monitored over time with anti-FLAG antibody. Pgk1 was used as a loading control. The experiment was repeated three times and the relative abundance of Huntingtin over Pgk1 is shown in **C** as mean ± SD. The Wilcoxon rank sum test was used to calculate *p*-values, and the difference was considered significant (*) when $p < 0.05$.

Figure S2 (related to Figure 3). Increased Hsp104-positive aggregates in *cdc48-3*, *npl4-1*, and *ufd1-2* mutants. **A.** WT (YYW315-2) and *cdc48-3* (3506-1-1) mutants containing *HSP104-GFP* were grown in YPD (glucose medium) to mid-log phase at 25°C. Cells were then shifted to 34°C for 3 hours. Hsp104-GFP foci in WT and mutant cells were imaged (left) and quantified (right). The result is the average from three independent experiments (mean ± SD). Two-way ANOVA analysis with Tukey's multiple comparison test was performed (N = 3). *, $p < 0.05$; **, $p < 0.01$. Scale bar = 5μm. **B.** The Hsp104-GFP signal in WT (YYW316-1), *npl4-1* (3641-2-2), and *ufd1-2* (3642-1-1) mutants was compared using the same protocol as in (A).

Figure S3 (related to Figure 4). The accumulation of Htt103QP on the proteasome increases in *cdc48-3* mutants. WT (3589-1-4), *RPN11-3×FLAG P_{GAL}-Htt103QP-GFP* (3592-3-3), and *cdc48-3 RPN11-3×FLAG P_{GAL}-Htt103QP-GFP* (3592-3-1) cells (80 mL) in *pdr5*Δ background were grown in YPR (raffinose medium) to mid-log phase at 25°C. Cells were shifted to 34°C and galactose was added for 3 hours. The proteasome inhibitor, MG132, was then added for 1 hour. Cells were harvested and lysed, and Rpn11-3×FLAG protein was immunoprecipitated using M2 anti-Flag beads. Htt103QP-GFP was detected using anti-GFP antibody. A 4% SDS-PAGE was

used to visualize Htt103QP-GFP species associated with proteasome protein Rpn11. In the strains used in this experiment, the Htt103QP construct lacked the FLAG tag that is present in most other experiments.

Figure S4 (related to Figure 4). Deletion of *SAN1* and *UBR1* deletion partially suppresses the accumulation of ubiquitinated proteins on proteasomes. Strains with the indicated genotypes (in *pdr5*Δ background) were grown in YPD (glucose medium) to mid-log phase and then shifted to 34°C for 3 hours. MG-132 (50 μM) was then added for 1 hour. The cells were lysed and Rpn11-3×FLAG protein was immunoprecipitated using M2 anti-FLAG beads and ubiquitinated proteins were detected using anti-Ub antibody. We used 4% SDS-PAGE to visualize ubiquitinated high-molecular-weight protein species. A *pdr5*Δ strain (3589-1-4) was used as a negative control. *cdc48-3* (3592-3-1), *san1*Δ *ubr1*Δ (3625-1-2), and two *cdc48-3 san1*Δ *ubr1*Δ strains (3622-1-3 and 3624-1-1) were used to examine the level of high-molecular-weight species that are associated with proteasome protein Rpn11. These strains contain *RPN11-3×FLAG* and P_{GAL}*Htt103QP-GFP* that lacks the N-terminal FLAG tag. In this experiment, yeast cells were grown in glucose medium and no Htt103QP expression is induced.

Figure S5 (related to Figure 4). The increased accumulation of ubiquitinated proteins on proteasomes in *cdc48-3* mutant cells depends on Dsk2 and Rad23. Yeast strains WT (3589-1-4), *RPN11-3×FLAG* (3592-4-4), *cdc48-3 RPN11-3×FLAG* (3592-5-2), and *cdc48-3 rad23*Δ *dsk2*Δ *RPN11-3×FLAG* (3967-2-4) in *pdr5*Δ background were grown in YPD (glucose medium) to mid-log phase and then shifted to 34°C for 3 hours. Proteasome inhibitor MG-132 was then added at 50 μM for 1 hour. The cell lysates were immunoprecipitated using M2 anti-FLAG beads for Rpn11-3×FLAG protein, and ubiquitinated protein species were detected using anti-Ub antibody. We used 4% SDS-PAGE to visualize ubiquitinated high-molecular-weight protein species. The protein levels of Rpn11-3×FLAG and Pgk1 are shown.

Figure S6 (related to Figure 5). **A.** Western blotting results show HA-Ub induction after switch from raffinose (Raff) to galactose (Gal) using anti-HA antibody. * indicates the HA-fusion peptide generated from the control vector. **B.** High-level ubiquitin expression in *cdc48-3* mutants. A empty vector (pRS416) or a P_{ADH1}*RPS31(UBI3)* ubiquitin plasmid was introduced into WT (Y300) and *cdc48-3* (MHY3512) cells, and the transformants were selected on URA dropout plates. Saturated

cultures of the transformants were serially 10-folded diluted and spotted onto URA dropout plates. Images were acquired after incubation at 25°C, 30°C, 34°C and 37°C for 3 days.

Figure S1. Higgins et al.

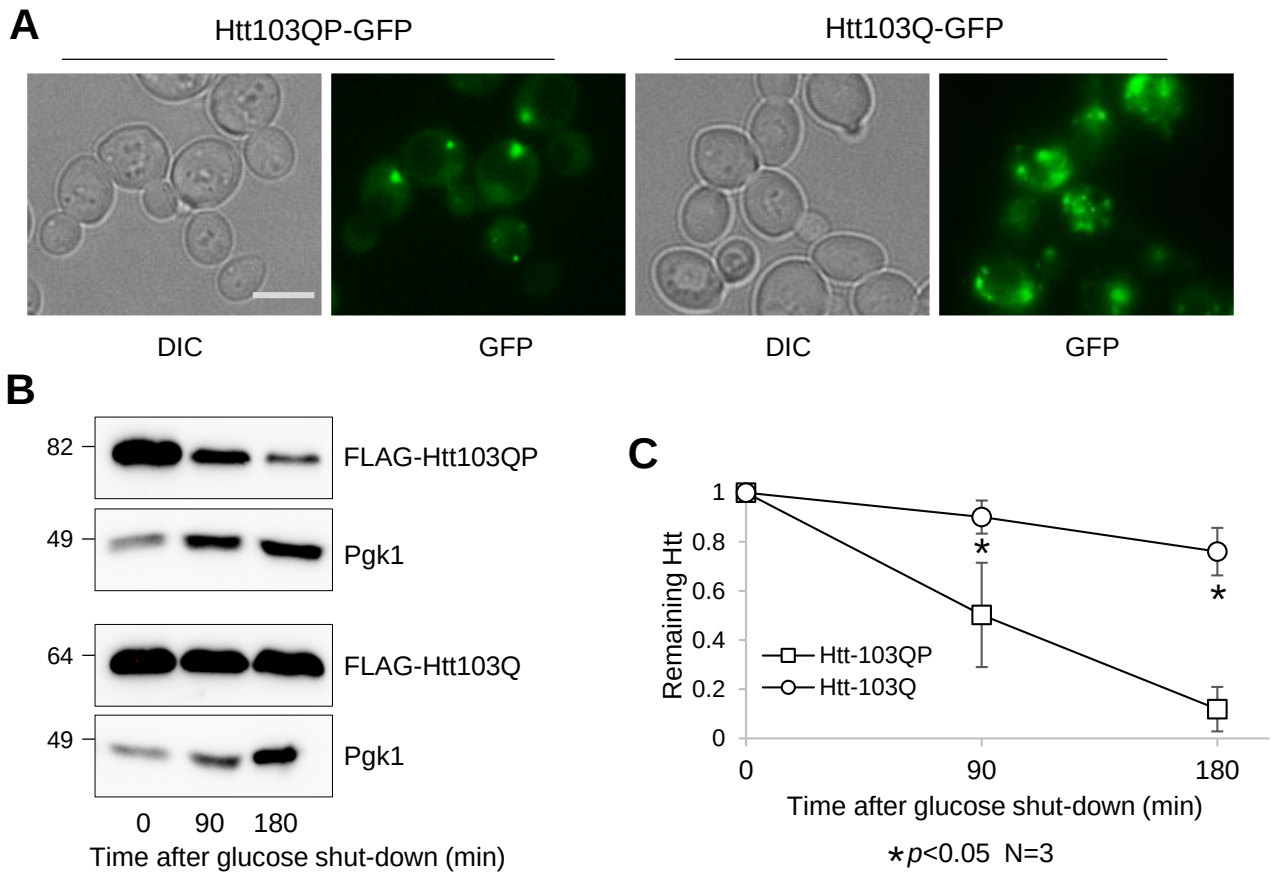

Fig. S2 Higgins et al.

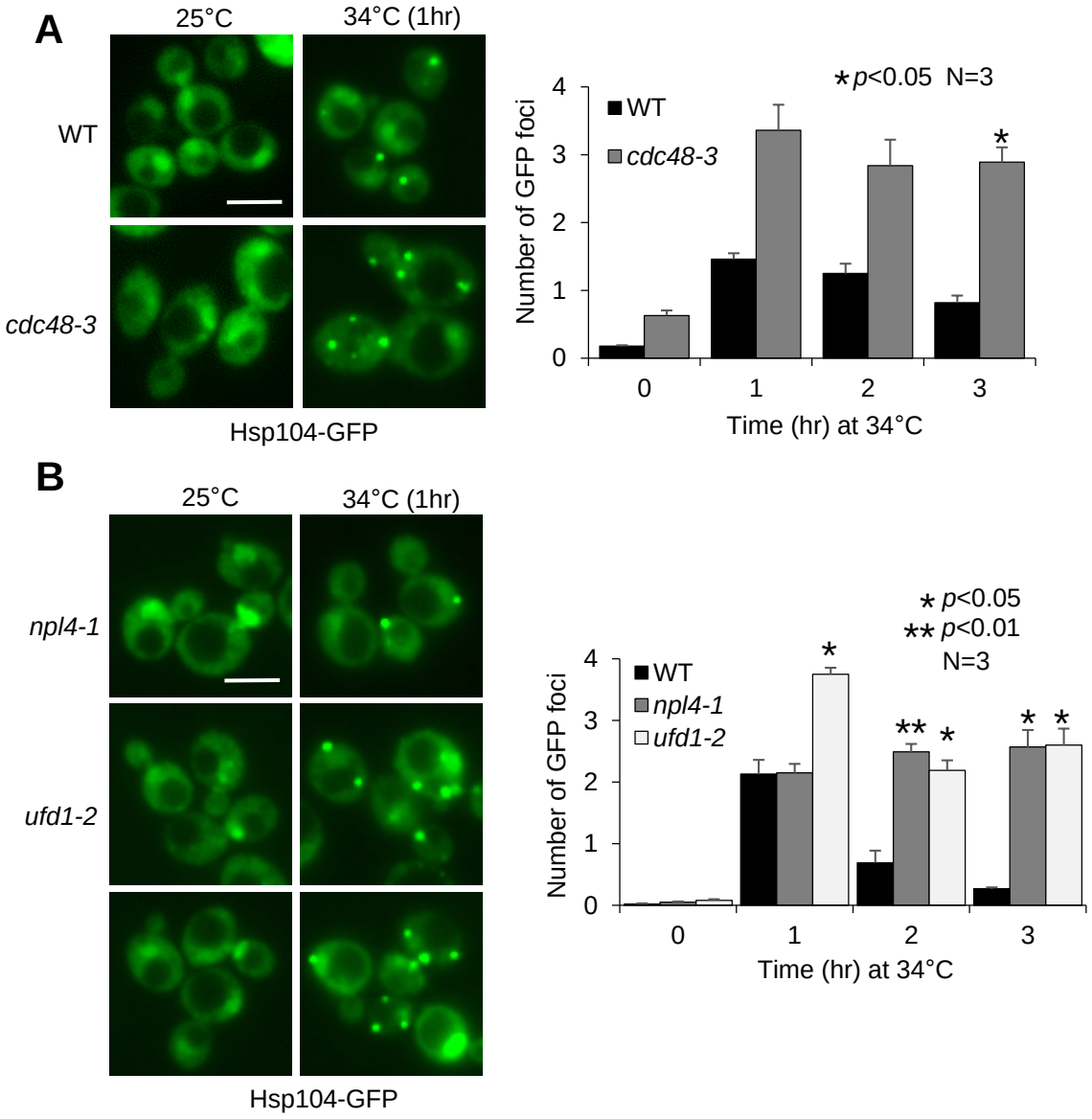

Figure S3. Higgins et al.

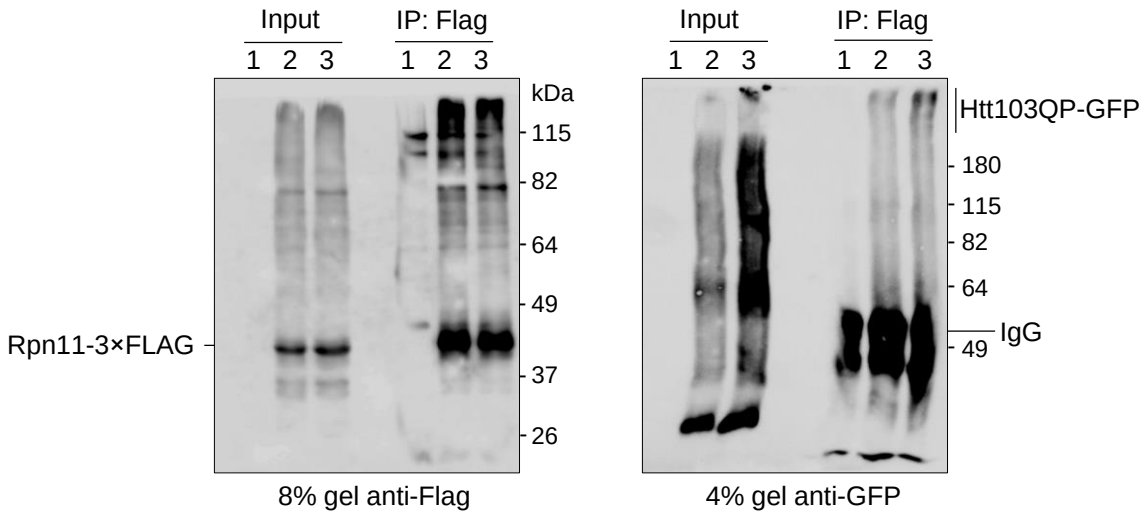

1. WT
2. *Rpn11-3×Flag Htt103QP-GFP*
3. *cdc48-3 Rpn11-3×Flag Htt103QP-GFP*

Figure S4. Higgins et al.

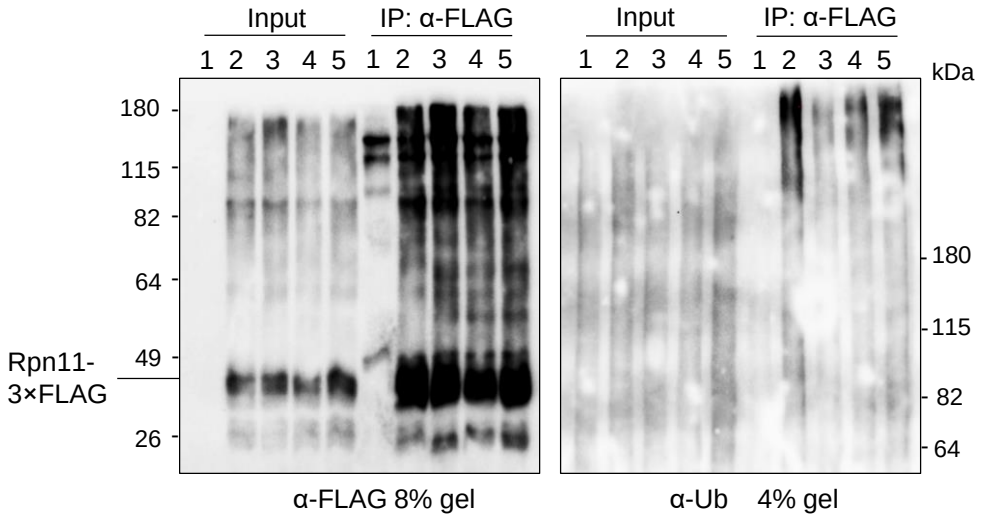

1. WT; **2.** *cdc48-3 RPN11-3×FLAG;* **3.** *san1Δ ubr1Δ RPN11-3×FLAG;* **4.** *san1Δ ubr1Δ cdc48-3 RPN11-3×FLAG;* **5.** *san1Δ ubr1Δ cdc48-3 RPN11-3×FLAG*

Figure S5. Higgins et al.

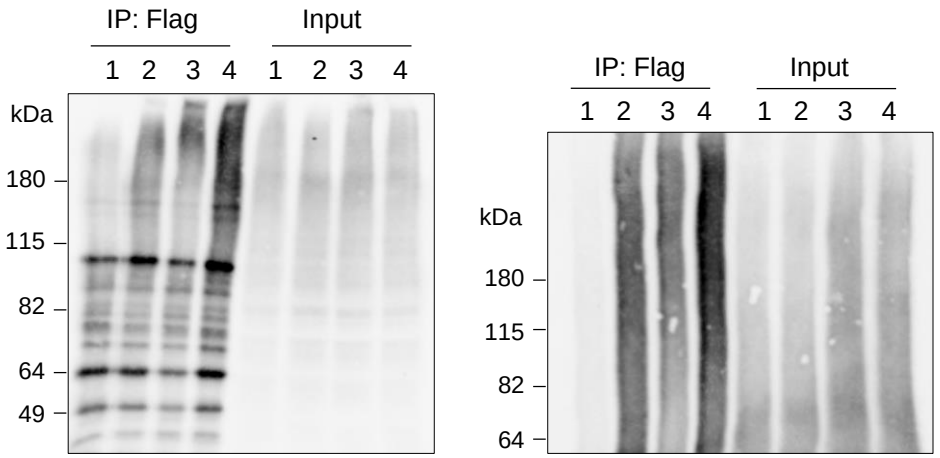

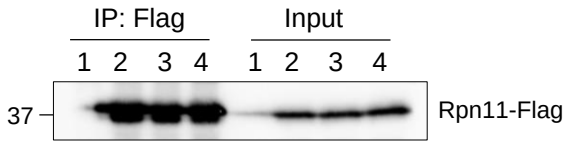

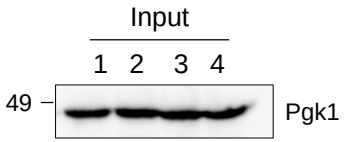

1: WT
2: *RPN11-3×FLAG*
3: *cdc48-3 dsk2Δ rad23Δ RPN11-3×FLAG*
4: *cdc48-3 RPN11-3×FLAG*

Figure S6. Higgins et al.

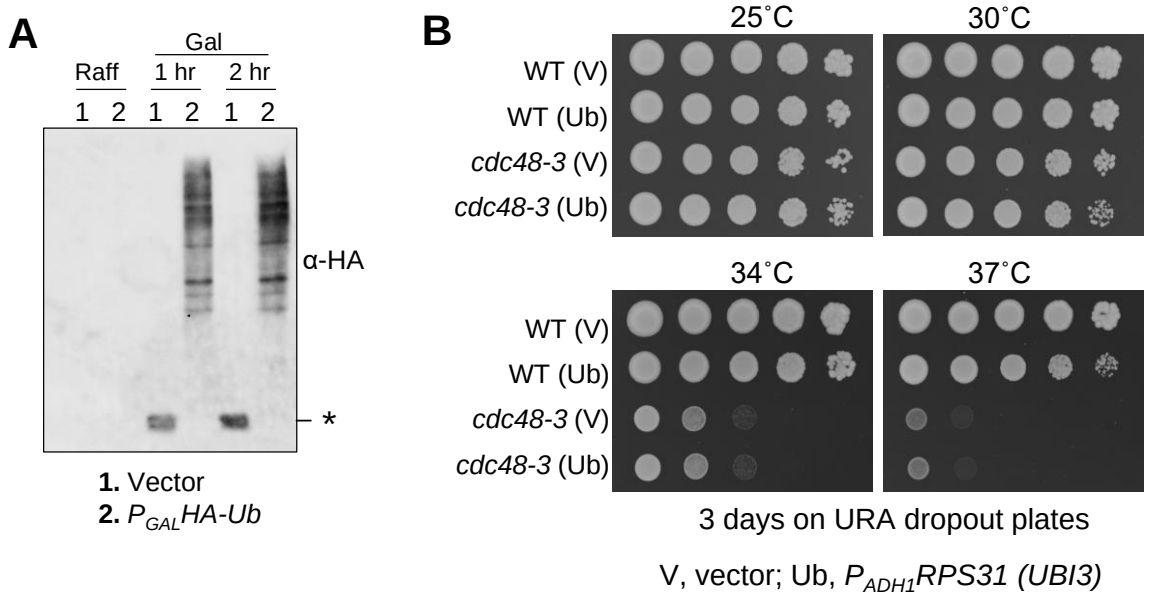

Table S1. Yeast deletion mutants used to screen the E3 ligase for Htt103QP (related to Figure 2A)

ORF	NAME	Motif
YAL002W	VPS8	RING finger
YBR062C	YBR062C	RING finger
YBR114W	RAD16	RING finger
YBR158W	AMN1	F-box
YBR203W	COS111	F-box
YBR280C	SAF1	F-box
YCR066W	RAD18	RING finger
YDL013W	SLX5	RING finger
YDL190C	UFD2	U-box
YDR049W	VMS1	Zinc finger, C2H2
YDR103W	STE5	RING finger
YDR131C	YDR131C	F-box
YDR132C	MRX16	BTB
YDR143C	SAN1	RNF-ring finger
YDR219C	MFB1	F BOX
YDR255C	RMD5	RING finger
YDR265W	PEX10	RING finger
YDR266C	HEL2	RING finger
YDR306C	PFU1	F-box
YDR313C	PIB1	RING finger
YDR457W	TOM1	HECT
YER116C	SLX8	RING finger
YGL003C	CDH1	WD40 repeat, APC/C complex component
YGL131C	SNT2	RING finger
YGL141W	HUL5	HECT
YGR003W	CUL3	CULLIN REPEAT
YGR184C	UBR1	RING finger
YHL010C	ETP1	RING finger
YHR115C	DMA1	RING finger
YIL001W	YIL001W	BTB
YIL030C	SSM4 (DOA10)	RING finger
YJL047C	RTT101	CULLIN
YJL149W	DAS1	F BOX
YJL157C	FAR1	RING finger
YJL204C	RCY1	F BOX
YJL210W	PEX2	RING finger
YJR036C	HUL4	HECT
YJR052W	RAD7	F-box
YJR090C	GRR1	F-box
YKL010C	UFD4	HECT
YKL034W	TUL1	RING finger
YKR017C	HEL1	RING finger
YLR024C	UBR2	RING finger
YLR032W	RAD5	RING finger

YLR097C	HRT3	F-box
YLR108C	YLR108C	BTB
YLR224W	UCC1	F-box
YLR247C	IRC20	RING finger
YLR352W	LUG1	F-box
YLR368W	MDM30	F-box
YLR427W	MAG2	RING finger
YML068W	ITT1	RING finger
YML088W	UFO1	F-box
YMR026C	PEX12	RING finger
YMR119W	ASI1	RING finger
YMR247C	RKR1	RING Zinc finger
YMR258C	ROY1	F-box
YNL008C	ASI3	RING finger
YNL023C	FAP1	RING finger
YNL116W	DMA2	RING finger
YNL230C	ELA1	F-box
YNL311C	SKP2	F-box
YOL013C	HRD1	RING finger
YOL054W	PSH1	RING finger
YOL138C	RTC1	RING finger
YOR080W	DIA2	F-box
YOR191W	ULS1	RING finger
YPL046C	ELC1	ELONGIN C,BTB,SKP1 COMPPNENT
YPR093C	ASR1	RING finger
YMR247C	RKR1	RING finger
YMR080C	NAM7	CH-rich domain (RING-related domain)

Table S2. Yeast strains used in this study (related to Star Methods)

Strains	Genotype	Reference
Y300 (WT)	Mata *ura3-1, his3-11,15 leu2-3,112 trp1-1, ade2-1, can1-100*	Lab Stock
MHY3512	Mata *cdc48-3 ura3-52 leu2-3, 122 ade2-1 trp1-1 his3*	Hochstasser
1126	Mata *npl4-1*	R.H. Chen
1122	Mata *ufd1-2*	R.H. Chen
3419-1-1	Mata P_{GAL}*FLAG-Htt103QP-GFP::URA3*	This study
3598-2-3	Mata *cdc48-3* P_{GAL}*FLAG-Htt103QP-GFP::URA3*	This study
3387-3-4	Mata *npl4-1* P_{GAL}*FLAG-Htt103QP-GFP::URA3*	This study
3385-4-4	Mata *ufd1-2* P_{GAL}*FLAG-Htt103QP-GFP::URA3*	This study
RH142	Mata *san1::Sphis5*$^+$ P_{GAL}*FLAG-Htt103QP-GFP::URA3*	This study
3301-2-2	Mata *san1::KanMX* P_{GAL}*FLAG-Htt103QP-GFP::URA3*	This study
3522-4-4	Mata *ubr1::KanMX* P_{GAL}*FLAG-Htt103QP-GFP::URA3*	This study
3287-1-1	Mata *ltn1::KanMX* P_{GAL}*FLAG-Htt103QP-GFP::URA3*	This study
3288-1-3	Mata *ufd2::KanMX* P_{GAL}*FLAG-Htt103QP-GFP::URA3*	This study
2925-3-2	Mata *HTA1-mApple-HIS3* P_{GAL}*FLAG-Htt103QP-GFP::URA3*	This study
3222-1-1	Mata *dsk2::TRP1* P_{GAL}*FLAG-Htt103QP-GFP::URA3*	This study
3514-1-2	Mata *dsk2::TRP1 san1::KanMX* P_{GAL}*FLAG-Htt103QP-GFP::URA3*	This study
FY-13-1	Mata Y300 (P_{GAL}*HA-CLB5::URA3)*	This study
3504-3-2	Mata *cdc48-3* (P_{GAL}*HA-CLB5::URA3*)	This study
3580-1-3	Mata *cdc48-3 san1::TRP1 ubr1::Sphis5*$^+$ (P_{GAL}*HA-CLB5::URA3*)	This study
3660-1-4	Mata *cdc48-3 ubr2::KanMX* (P_{GAL}*HA-CLB5::URA3*)	This study
229-3-2	Mata *CLB5-HA*	Lab stock
3968-4-3	Mata *cdc48-3 san1::TRP1 ubr1::Sphis5*$^+$ *CLB5-HA*	This study
3968-5-1	Mata *cdc48-3 CLB5-HA*	This study
3969-4-4	Mata *ubr2::KanMX*	This study
3655-2-4	Mata *cdc48-3 ubr2::KanMX*	This study
3658-1-4	Mata *npl4-1 ubr2::KanMX*	This study
3659-1-2	Mata *ufd1-2 ubr2::KanMX*	This study
3550-5-3	Mata *cdc48-3 san1::TRP1*	This study
3550-6-3	Mata *cdc48-3 ubr1::Sphis5*$^+$	This study
3550-2-1	Mata *cdc48-3 san1::TRP1 ubr1::Sphis5*$^+$	This study
3555-5-1	Matα *npl4-1 san1:TRP1 ubr1::Sphis5*$^+$	This study
3556-3-3	Mata *ufd1-2 san1:TRP1 ubr1::Sphis5*$^+$	This study
3556-1-1	Mata *ufd1-2 san1::TRP1*	This study
3556-2-3	Mata *ufd1-2 ubr1::Sphis5*$^+$	This study
YYW14	Mata *dsk2::TRP1*	This study
3553-2-4	Mata *rad23::Sphis5*$^+$	This study
3553-5-3	Mata *dsk2:TRP1 rad23::Sphis5*$^+$	This study
3553-10-3	Mata *cdc48-3 rad23::Sphis5*$^+$	This study
3553-7-2	Mata *cdc48-3 dsk2::TRP1*	This study
3553-3-2	Mata *cdc48-3 rad23::Sphis5*$^+$ *dsk2::TRP1*	This study
RH156	Mata Y300 (*p1217*, empty vector *TRP1*)	This study
RH157	Mata Y300 (P_{GAL}*HA-Ub-TRP1)*	This study
RH158	Mata *cdc48-3* (*p1217*, empty vector *TRP1*)	This study
RH159	Mata *cdc48-3* (P_{GAL}*HA-Ub-TRP1)*	This study
RH160	Mata *npl4-1* (*p1217*, empty vector *TRP1*)	This study
RH161	Mata *npl4-1* (P_{GAL}*HA-Ub-TRP1)*	This study
RH162	Mata *ufd1-2* (*p1217*, empty vector *TRP1*)	This study
RH163	Mata *ufd1-2* (P_{GAL}*HA-Ub-TRP1)*	This study
3589-1-4	Mata *pdr5::KanMX*	This study
3592-4-4	Mata *pdr5::KanMX RPN11-3×FLAG::HIS3*	This study
3592-5-2	Mata *pdr5::KanMX cdc48-3 RPN11-3×FLAG::HIS3*	This study

3592-3-1	Mata *pdr5::KanMX cdc48-3 RPN11-3×FLAG::HIS3* P_{GAL}*Htt103QP-GFP::URA3*	This study
3592-3-3	Mata *pdr5::KanMX RPN11-3×FLAG::HIS3* P_{GAL}*Htt103QP-GFP::URA3*	This study
3625-1-2	Matα *pdr5::KanMX san1::TRP1 ubr1:: Sphis5*$^{+}$ *RPN11-3×FLAG::HIS3* P_{GAL}*Htt103QP-GFP::URA3*	This study
3622-1-3	Mata *pdr5::KanMX cdc48-3 san1::TRP1 ubr1:: Sphis5*$^{+}$ *RPN11-3×FLAG::HIS3* P_{GAL}*Htt103QP-GFP::URA3*	This study
3624-1-1	Mata *pdr5:Kan cdc48-3 san1::TRP1 ubr1::Sphis5*$^{+}$*RPN11-3×FLAG::HIS3* P_{GAL}*Htt103QP-GFP::URA3*	This study
3967-2-4	Mata *pdr5:Kan cdc48-3 dsk2::TRP1 rad23::Sphis5*$^{+}$*RPN11-3×FLAG::HIS3*	This study
YYW315-2	Mata *HSP104-GFP::TRP1*	This study
3506-1-1	Mata *cdc48-3 HSP104-GFP::TRP1*	This study
YYW316-1	Mata *HSP104-GFP::Sphis5*$^{+}$	This study
3641-2-2	Mata *npl4-1 HSP104-GFP::Sphis5*$^{+}$	This study
3642-1-1	Matα *ufd1-2 HSP104-GFP::Sphis5*$^{+}$	This study
YYW313-1	Matα P_{GAL}*Htt103Q-GFP::URA3*	This study
PHY648	Mata *ppz1::KANMX ppz2::NATMX*	MacGurn lab
4023-1-1	Mata *cdc48-3 ppz1::KANMX*	This study
4023-2-4	Mata *cdc48-3 ppz1::KANMX ppz2::NATMX*	This study
4023-8-4	Matα *cdc48-3 ppz1::KANMX ppz2::NATMX*	This study